UNIVERSITY OF OSLO
Department of Geosciences
MetOs section

Performance of the global EMEP model in Asia

Master thesis in Geosciences Meteorology and Oceanography

Anne Solveig Håvelsrud Andersen

8 June 2009

Abstract

Air pollution is a great danger to our health and nature. Asia has the latest decades had a rapid increase in population and industrialization, affecting not only Asia, but also other parts of the world. The main focus in this thesis is air pollution in Asia by evaluating the global EMEP model performance in this area.

The global EMEP model performance over Asia has been validated with the use of observations from EANET (Acid Deposition Monitoring Network in East Asia). The comparison distinguished between urban, rural and remote sites. And the global EMEP model shows better simulations in rural and remote sites. However, compared to the performance of European model simulation from the regional EMEP model, the global EMEP model show high underestimations of SO_2 and NO_2 concentrations over Asia. Model simulations of ozone were generally in better agreement with measurements.

To better understand effects of the emissions on model results, the global EMEP model was run with two different emission inventories over Asia. Both emission inventories were based on ACESS (Ace-Asia and Trace-P Modelling and Emission Support System) emissions. The main differences between the emission inventories were the allocation of emissions in source sectors. The original emissions showed to be placed mainly in the source sector S1, for road traffic, where the pollutants are emitted at the lowest layer of the atmosphere. The new emissions however, showed more detailed source sector distribution, with emissions in the four source sectors, S1; combustion in energy and transformation industries, S2; non-industrial combustion plants, S3; combustion in manufacturing industry, and S7; road transport. The new emissions gave a more realistic source distribution and therefore also vertical distribution of the emissions.
Comparing the two model results showed a substantial increase in the long-range transport of SO_2, as much as 20 % and as far as North-America at 650 meters height. This caused by releasing the emissions at higher levels. Evaluating the differences in model results for SO_2, NO_2 and O_3 at a level above the boundary layer, showed the model run with new sector distribution to be more sensitive to long-range transport for all pollutants analysed. Temporal correlations with observations were improved in the model run with new emissions for all pollutants, with increase in mean correlation of 0.017, 0.022 and 0.019 for SO_2, NO_2 and O_3 concentrations, respectively. However, the new emissions did generally not improvement in the model simulations of the surface air concentrations of SO_2 and NO_2.

The global EMEP model performance in Asia was also analysed against eight regional models included in a model study in the area, MICS-II. The comparison showed the global EMEP model to be in the same range as the regional models included in the model study for all pollutants analysed.

Acknowledgements

First of all I would like to thank my supervisor Leonor Tarrasón, for guidance and support throughout this thesis work, and for taking time to see me in a busy schedule.
A thank you to the people working at EMEP. Especially Semeena Valiyaveetil, for helping me with data processing and difficulties through the work. To Peter Wind, thank you so much for helping me with running the model and answering all my questions regarding the EMEP model. Thanks also to Heiko Klein for the use of his programmes and helping me with problems related to data processing. Also a thank you to Hilde Fagerli and Jan Eiof Jonson for tips and recommendations.
A thank you to my co-supervisor Frode Stordal for taking time to see me when it was needed. And to Gunnar Wollan at MetOs section for help me with fortran programming.
I would like to thank Senior Researcher Wenche Aas at NILU, for making the observation data from EANET available and for answering my questions regarding observation data.

To all my fellow students; I am grateful for all the support, cheering up and making the working day so much better. And a special thanks to Silje and Haldis for proof-reading and commenting my thesis.
Finally a special and important thank you to my great family and loved ones for keeping my spirit up and being there for me.

Contents

Chapter 1

Introduction

1.1 Background

Air pollution represent a health danger for people living in the affected areas. Air pollution from industry, traffic, energy production and other sources are a threat to us and our nature.
The ecosystems are harmed by contamination of the soil, which can damage forests, lakes, rives, wetlands etc. Air pollutants like sulphur and nitrogen compounds leads to acidification and alters the balance between, and budgets of soil nutrients.
For long air pollution has been recognised to lead to various illnesses from just a cold to more serious diseases like respiratory infections, mutations or fetus deformation (Informasjonsgruppen Mot Sur Nedbør, 1987).
The different air pollutants affect our health in many ways, some more damaging than others. Sulfur dioxide (SO_2) and nitrogen oxides (NO_x) seem to correlate with higher risk for diseases in the respiratory passages. Increasing cases of cancer can be a factor influenced by NO_x concentration. Different studies have shown that people living in areas with high levels of NO_x, especially from cars and other vehicles, may have their lung cancer risk increased by about a third (Cancer Research UK, 2009). Carbon monoxide (CO) can affect the heart and the central nervous system by restraining oxygen delivery to the blood and the body's organs and tissues. At extreme levels CO can be poisonous and cause death (Environmental Protection Agency, 2008). Ozone (O_3) can damage lungs and irritate the respiratory system, especially for children, people with lung diseases and people who perform outdoor activities.

The World Health Organisation, WHO, has warned that the citizens in the major cities in the Western Pacific Region, where the pollution is very high, will suffer dramatically unless urgent measures are taken. According to the WHO there is more than half a million people that die in Asia every year from diseases related to air pollution.

In the last few decades Asia has had a rapid population and economic growth and this has led to a development in anthropogenic emissions of air pollution. According to Pochanart et al. (2004) is the continuing rapid industrialization expected to make East Asia the largest source region for air pollution in the coming decades. About 60 percent of the worlds population of 6 billion people live in Asia. The development in population, industry and centralization is associated with growing use of energy, and this threatens the urban air quality. According to Ohara et al. (2007), SO_2 emissions in Asia between 1980 and 2000 have increased from 23 to 42 Tg/yr. NO_x emissions have increased from 11 to 25 Tg/yr, CO from 207 to 305 Tg/yr, and NMVOC (non-methane volatile organic compounds) from 22 to 40 Tg/yr. The increase in emissions are

significant, for NO_x the percentage emission increase is 135 %.
The area is of special interest since the developments in this region will deeply affect not only Asia, but also rest of the world. Long-range transport can bring air pollutants like O_3, SO_2 and its resultant aerosols from Asia and to other continents. Model studies and observations show that transport of Asian emissions influence the Northern Hemisphere, reach over the Pacific to North-America and also Europe (Pochanart et al., 2004; Collins et al., 2000; Jonson et al., 2001; Derwent et al., 2008). Europe is affected by the Asian emissions, for instance, according to Auvray and Bey (2005), does Asian O_3 contribute with 7,7% to the annual O_3 budget over Europe.

In contrast with Asian pollution growth have the European and North-American anthropogenic emissions of SO_2 and also NO_x, CO and NMVOC, all precursors of O_3, all decreased in the last decades. The realization of the impact of long-range transport turned the vision towards other continents, and especially Asia with the understanding of emissions and impacts of air quality in North-America and Europe. Modelling air quality is a tool for understanding the sources and reactions of the pollution, and in this way suggesting the best alternative to reduce pollution levels and to investigate how the long-range transport impact certain areas.

The Convention on Long-range Transboundary Air Pollution, CLRTAP, started in 1979 investigating environmental problems in United Nations Economic Commission for Europe, UNECE, region. In 2001 a Task Force was established concerning the long-range transport issue; Task Force in Hemispheric Transport of Air Pollutants, TFHTAP. The EMEP programme is a part of CLRTAP and the global EMEP model evaluated in this thesis was developed as a result of the Task Force in Hemispheric Transport of Air Pollutants. The regional EMEP model has been validated in Europe for several years, however the first evaluation of the global EMEP model, (Jonson et al., 2007), showed poor model results over Asia, with uncertainties like emission data.

Knowledge about the emissions is an important part of understanding and estimating air pollution. The skills of a model depends on its input data, therefore the emission input is of great importance.
In Asia there is considerable uncertainties with some of the emission values. The reasons can be lack of national statistics in some Asian countries, and also insufficient knowledge of the performance of some of the emitters. According to Streets et al. (2003), CO emissions depend on the efficiency of the combustion process, and how the equipment used are operated and maintained. These aspects are difficult to get an statistic view over.
The best known pollutant emitted in Asia is SO_2. The reason for this is associated with the threat of acid rain becoming a concern in the early 1990s, and researchers in Japan started then studies of SO_2 emissions. However estimates of pollutants like NO_x, CO, CO_2 (carbon dioxide), CH_4 (methane) and NMVOC (non-methane volatile organic compounds) are estimated with uncertainties, (Streets et al., 2003). There are, especially for some areas of Asia, few estimates to compare against and often from different time periods. The inventories often include or exclude different sources, which makes the comparison difficult.

For valid analyses of the effects of long-range transport of Asian emissions to North-America and Europe, the Asian pollution must be understood. The fate of the pollutants in the atmosphere, and how the long-range transport will impact pollution levels in other locations have been a subject of interest. An intercomparison study of chemical transport models in East Asia was conducted by Carmichael et al. in 2001, MICS-I, and an expanded version in 2003, MICS-II, (Carmichael et al., 2007). According to Carmichael et al. (2007) the study was conducted to

help develop a better common understanding of the performance and uncertainties of chemical transport models in East Asia. The study included nine regional, three-dimensional Eulerian models over four different periods, including three different seasons and two years; March, July and December in 2001, and March in 2002. The models studied deposition of sulfur and nitrogen compounds, O_3 and aerosols. The seasons where analysed and compared to observations in EANET, Aid Deposition Monitoring Network in East Asia, sites in East Asia. Results showed significant differences, but the tendencies are overprediction of SO_2, and underprediction of NO_2 and O_3 (Han et al., 2007). The comparison study is a benchmarking for chemical transport modelling in this area and gives a foundation of the analysis for the global EMEP model evaluated in this thesis.

The global EMEP model has recently been developed (2007) and this thesis provides for the first time a thorough evaluation of the model performance over Asia. The model results are evaluated for the air pollutants SO_2, NO_2 and O_3. The reason for this focus is the rising concern of acid rain in Asia from the early 1990s. EANET, was initiated in 1998 and started monitoring activities in 2001. Air concentrations were measured for SO_2, NO_2, NO, O_3 ad PM. The observations are a basis of comparison against the global EMEP model results in Asia.

1.2 Purpose of the thesis

The purpose of this thesis is to get a better understanding of the air quality in Asia. In particular to document the performance of the global EMEP model, and to give recommendations for improvements in the model results over Asia. The global EMEP model is run with different emission inventories and the models performance influenced by changes in emission data are evaluated.

This thesis is organized in 6 chapters. First the global EMEP model is introduced. In the next chapter, chapter 3, a description of the observations used for model validation over Asia is presented, providing an understanding of their location and classification. The emission input used in this thesis is presented and discussed in chapter 4. The emission data from ACESS, Ace-Asia and Trace-P Modelling and Emission Support System, are analysed with emphasis on the source sector distribution. Chapter five evaluated the global EMEP models performance in Asia, with validation of model results against observation data from EANET and against other model results in Asia, MICS-II. The two last chapters contains discussion, and conclusions with recommendations for improvements of the global EMEP model performance in Asia.

Chapter 2

The EMEP Chemical Transport Model

2.1 The EMEP programme

EMEP stands for “Co-operative programme for monitoring and evaluation of the long-range transmission of air pollutants in Europe”, and is a scientifically based and policy driven programme under the Convention on Long-range Transboundary Air Pollution for international co-operation to solve transboundary air pollution problems, (EMEP, 2009).

CLRTAP started in 1979 and has investigated some of the environmental problems of the UN-ECE region. The Convention has now 51 Parties and the goal is that the Parties shall attempt to limit and gradually reduce and prevent air pollution, including long-range transboundary air pollution. There are three main programmes under CRLTAP; the Working Group on Effects, EMEP and the Working Group on Strategies and Review, these all report to the Executive Body every year as well as the Convention’s Implementation Committee, (UNECE, United Nations Economic Commission of Europe, 2009).

The EMEP programme provides the Convention with information on atmospheric monitoring and modelling, emission inventories and emission projections, and integrated assessment modelling. The main purpose of the EMEP programme is to provide information on the origin of long-range transboundary air pollution. The programme is based on international cooperation in compiling emission data, observations and modelling. This gives a basis for evaluation and qualification of the EMEP estimates.

The EMEP programme is organised in five different centers in Europe; in Oslo, and under the Norwegian Meteorological Institute is the MSC-W, Meteorological Synthesizing Centre - West, there are also a centre in the east, in Moscow, MSC-E, a Chemical Coordinating Centre (CCC) hosted by NILU, a Centre for Integrated Assessment Modelling (CIAM) and a Centre on Emission Inventories and Projections (CEIP).
Within EMEP there are four Task Forces; the Task Force on Measurements and Modelling (TFMM), the Task Force on Emission Inventories and Projections (TFEIP), the Task Force in Integrated Assessment Modelling (TFIAM) and the Task Force in Hemispheric Transport of Air Pollutants (TFHTAP).
CCC provides recommendations of measurements, while MSC-West have the modelling responsibility, for sulphur, nitrogen photooxidants pollutants, particles in the atmosphere. MSC-East has the responsibility for development of modelling for heavy metals and POPs. In 1999 CIAM and CEIP where included in the Convention. CIAM stands for integrated assessment, building

on past modelling work, especially on the RAINS model. CEIP collects emissions and projections of acidifying air pollutants, heavy metals, particulate matter and photochemical oxidants, (EMEP, 2009).
The Task Force HTAP was established by the Convention in 2001, with the assignment to determine the extent and impacts of intercontinental transport of air pollution, and also focus on improving trans-continental co-operation to reduce air pollution.
This was the reason for the extension of the Unified EMEP model that was originally validated in Europe. MSC-West has in the last few years been developing the Unified EMEP model that has a flexible modelling system capable of bridging different scales, from local to regional, hemispheric and global, (Jonson et al., 2007). The first step towards the global model was a hemispheric model, the first model results were presented in Jonson et al. (2006). In 2007, for the first time the results from the global model were presented in Jonson et al. (2007). These results presented a preliminary evaluation of the global EMEP model performance in Asia. However this thesis brings forward a more detailed evaluation of the global EMEP model in Asia.

2.2 The global EMEP model

The Unified EMEP model is a Eulerian atmospheric dispersion model with multiple vertical layers. It is used primarily for simulating long-range transport of air pollution. The global EMEP model is an extension of the regional EMEP model. The global and regional model share the same formulations, except for the grid projection and input data, that is the meteorology, the emissions and the description of land cover. The grid resolution in the global model is 1° x 1° ($\sim$ 110 x 110 km^2), while the regional model has a finer resolution of 50 x 50 km^2. The projection for the global model is in longitude-latitude, while the regional model used a polar stereographic projection. The input data is discussed in subsection 2.2.2 in this chapter.

2.2.1 Model description

The EMEP model is a chemical transport model (CTM), a numerical model that simulates atmospheric transport and chemistry. The chemical transport model solves the continuity equation for the species, and the processes included in the equation are emissions, transport, chemical transformation and removal of the species.

The Unified EMEP model is an Eulerian model. An Eulerian frame reference describe the fluid motions by focusing on specific locations in space, where the fluid flows through. By contrast a Lagrangian model is looking at fluid motion where the observer follows the individual particles as they move around in time and space.
A continuity equation is a differential equation that describes the conservative transport of some kind of quantity. Since mass, energy, momentum, and other natural quantities are conserved, a vast variety of physics may be described with continuity equations.
The continuity equation used in the EMEP model, from EMEP Status Report 1/2003, (Simpson et al., 2003), is the equation given below. Here C is the mixing ratio (kg/kg-air) of any pollutant:

$$\frac{\partial}{\partial t}(Cp*) = -m^2\nabla_H \cdot (\frac{\mathbf{V}_H}{m}(Cp*)) - \frac{\partial}{\partial\sigma}(\dot{\sigma}Cp*) + \frac{\partial}{\partial\sigma}\left[K_\sigma\frac{\partial}{\partial\sigma}(Cp*)\right] + \frac{p*}{\rho}S \qquad (2.1)$$

The model uses σ-coordinates in the vertical, see equation 2.2, where p* = p_S - p_T. p, p_S and p_T is the pressure at the level σ, the surface and top of the atmosphere, respectively. There are

20 vertical levels, where the vertical numbering coordinate, k, is inverted. This means that k = 1 for the highest level, near 100 hPa, and k = 20 for the level near the surface.

$$\sigma = (\frac{p - p_T}{p*}) \tag{2.2}$$

The two first terms on the right side of the continuity equation 2.1 are the flux divergence formulation of the advective transport. Advection is the transport of a substance from one point to another, applied mostly to horizontal motion, but also important in the vertical in some cases, (Dunlop, 2001). The first term is the horizontal advection, where $\mathbf{V}_H$ and ∇_H are the horizontal wind vector and del operator, respectively. *m* is the map factor on a long/lat map projection. The second term is the vertical advection, where the vertical velocity is given by $\dot{\sigma} = \frac{d\sigma}{dt}$. Advection on the components in the model is numerically based on the Bott (1989) numerical scheme, (Simpson et al., 2003). The fourth order scheme is utilized in the horizontal directions. While a second order version applicable to variable grid distance used in the vertical directions.

The third term on the right hand side in equation 2.1 represents the vertical eddy diffusion, here K_σ is the gravitiational acceleration, air density and vertical eddy diffusion coefficient respectively (in σ-coordinates). Diffusion is the process where two gases or fluids become mixed trough molecular motion, (Dunlop, 2001). Diffusion is parameterized in the vertial according to K-theory and, only the vertical diffusion is considered.

The last term in the continuity equation includes chemical or other source and sink terms, *S*. In this term the sources can be emissions or chemical productions, and sinks can be chemical reactions or wet and dry deposition. EMEP chemical scheme, UNI-OZONE, has been used in the model, this scheme has been extensively peer-reviewed, (Andersson-Sköld and Simpson, 2001). 70 species and about 140 reactions are included in the Unified model, (Simpson et al., 2003). Particulate matter are divided into fine and coarse particles, fine; PM2.5 - particles with dry aerosol diameter smaller than 2.5 μm, and coarse; PMcoarse with diameter between 2.5 and 10 μm. The particulate components included in the simulations are secondary inorganic aerosols, like sulphate, nitrates and ammonium, and primary particle matter, mainly anthropogenic elemental carbon, organic carbon and dust. Natural sources of PM from biomass burning and natural dust emission is not explicitly included in the calculations.
Wet deposition is associated with precipitation, the gas or particles can be removed from the atmosphere by uptake into a drop. It involves all processes where airborne species are transferred to the surface in aqueous form, e. g. rain, snow or fog. Wet deposition will take place unevenly in time and space. Dry deposition to the surface can take place continuously, it depends on metorological conditions and is a direct transfer of species. Here both gasous and particulate species transfer to the surface and proceeds without precipitation, (Seinfeld J.H. and Pandis S.N., 1998). The dry deposition module used in the EMEP global model is based on the resistance analogy. The surface resistance is the most complex variable in the deposition model and it depends on the characteristics of the surface and chemistry of the species deposited. It is parametrized for the different components as described in Simpson et al. (2003).
Dry deposition is parameterized following a resistance approach including stomatal and non-stomatal resistances. Stomatal resistance is calculated with the multiplicative model of Emberson et al. (2000), and factors like maximum stomatal conductance, time of year (leaf phenology), the minimum observed stomatal conductance, light (actually photon flux density, PFD), leaf-temperature (T), leaf-to-air vapour-pressure deficit (VPD), and soil-water potential (SWP). For the non-stomatal perspective, the conductance for ozone has been extensively evaluated (Em-

berson et al., 2000; Tuovinen et al., 2001, 2004).
Wet depositions parameterized according to scaveging ratios and distinguishes between-cloud and sub-cloud scaveging without explicit dependence in the pH of precipitation.

In the Unified model other processes like horizontal eddy diffusion and convection terms are not included.
Emissions and boundary conditions in the EMEP model are combination of observations and predictions for future ozone levels based on ozone trend analysis, documented in Simpson et al. (2003).

2.2.2 Input data

The global EMEP model is an extension of the regional model, and the two model uses the same formulations, except for grid projection and input data; meteorology, emission data and land-use.

Emissions

Air concentrations of pollution are to a great extent determined by the emissions of its precursor gases and particles. Therefore, accurate emission estimates are essential to model calculations of air pollution. The emission data used by the Unified EMEP model is described in general terms below. In chapter 4 a detailed analysis of the emission input used in the global model is presented.

The emission information necessary for the EMEP model is: Information on emissions input data consisting of gridded emissions of sulphur dioxide (SO_2), nitrogen oxides (NO_x=NO+NO_2), ammonia (NH_3), non-methane volatile organic compounds (NMVOC), carbon monoxide (CO), and particulates ($PM_{2.5}$, PM_{10}). In Europe the information is in annual emission intensities per country and sector files, where the temporal distribution of the emissions are according to monthly, weekly and daily factors derived from data provided by the University of Stuttgart (IER), (Simpson et al., 2003). Outside Europe the model uses monthly emissions with daily variations described below in this chapter. For biogenic VOC emissions the global model uses temperature dependent emissions from forests, following the methodology of the regional EMEP model.

The EMEP model distributes the emissions in 11 source sectors. To specify sources of emissions are relevant for better understanding the origin of the air pollution, and in this way see the effect of the different emission sources. The information is highly useful for suggesting possible regulation and restrictions in emission sources.
The 11 source sectors have different specifications in temporal and spatial distribution. The classification of the sources are described in joint EMEP/CORINAIR Atmospheric Emission Inventory Guidebook, (EMEP/CORINAIR, 2000). CORINAIR, Core Inventory of Air Emissions, is a project by European Topic Centre of Air Emissions started in 1995. The goal of this project is to collect, maintain, manage and publish information on emissions into the air, by means of a European air emission inventory and database system, (Maes et al., 2009).
The Guidebook has been prepared by the expert panels of the UNECE/EMEP Task Force on Emission Inventories (TFEI), and it is intended for general reference and for use by parties to the Convention on Long Range Transboundary Air Pollution, (EMEP/CORINAIR, 2000). The first edition of the Guidebook was subsequently completed in 1996, and after that other editions

have been released.
The emissions are divided into 11 sources or SNAP sector, SNAP, Selected Nomenclature for sources of Air Pollution. The sectors were developed as a part of the CORINAIR project and they distinguish emission source sectors, sub-sectors and activities. A description of the sectors are given below and for more details see EMEP/CORINAIR (2000).

SNAP SECTORS according to EMEP/CORINAIR (2000):

S1: Combustion in energy and transformation industries (stationary sources)

- Public power, District heating plants, Petroleum refining plants, Solid fuel transformation plants and Coal mining, oil/gas extraction, pipeline compressors

S2: Non-industrial combustion plants (stationary sources)

- Commercial and institutional plants, Residential plants and Plants in agriculture, forestry and aquaculture

S3: Combustion in manufacturing industry (stationary sources)

- Combustion in boilers, gas turbines and stationary engines(Industry), Processes with or without contact(Industry-Iron and steel, Industry-Other, etc.)

S4: Production processes (stationary sources)

- Processes in petroleum industries, Processes in iron and steel industries and collieries, Processes in non-ferrous metal industries, Processes in inorganic chemical industries, Processes in organic chemical industries (bulk production), Processes in wood, paper pulp, food, drink and other industries and Production of halocarbons and sulphur hexafluoride

S5: Extraction and distribution of fossil fuel and geothermal energy

- Extraction and 1st treatment of solid fossil fuels, Extraction, 1st treatment and loading of liquid fossil fuels, Extraction, 1st treat. and loading of gaseous fossil fuels, Liquid fuel distribution (except petrol distribution), Petrol distribution, Gas distribution networks and Geothermal energy extraction

S6: Solvent use and other product use

- Paint application, Degreasing, dry cleaning and electronics, Chemical products manufacturing or processing and Other use of solvents and related activities

S7: Road transport

- Passenger cars, Light-duty vehicles < 3.5 t, Heavy-duty vehicles > 3.5 t and Buses, Mopeds and Motorcycles < 50 cm3, Motorcycles > 50 cm3, Gasoline evaporation from vehicles, Automobile tyre and brake wear and Automobile road abrasion

S8: Other mobile sources and machinery

- Military, Railways, Inland waterways, Maritime activities, Air traffic, Agriculture, Forestry, Industry, Household and gardening and Other off-road

S9: Waste treatment and disposal

- Waste incineration, Solid waste disposal on land, Open burning of agricultural wastes, Cremation and Other waste treatment

S10: Agriculture

- Cultures with fertilisers (fertilised agricultural land), Cultures without fertilisers, On-field burning of stubble, straw,..., Enteric fermentation, Manure management regarding Organic compounds, Use of pesticides and Limestone, Manure management regarding Nitrogen compounds and Fugitive PM sources

S11: Other sources and sinks

- Non-managed broadleaf forests, Non-managed coniferous forests, Forest and other vegetation fires, Natural grassland and other vegetation, Wetlands (marshes - swamps), Waters, Volcanoes, Gas seeps, Lightning, etc.

The distribution of emission in source sector effects the height variation and day/night varia-

tion of the emission input. The sectors height distribution used in the EMEP model is described in Table 2.1. The level where the emissions are released depends on the sources, for instance is pollution from an automobile emitted in lower altitudes than emission from an industry chimney. Low level emissions compared to emissions in higher altitudes are influenced differently by meteorology and chemical reactions. Like the effect of dry deposition being more valid in lower layers, and that emissions released at higher altitudes are more sensitive to long-range transport. According to Table 2.1, the EMEP model assume that the high level sources are mainly in S1, combustion in energy and transformation industries, S3, combustion in manufacturing industry, and S9, waste treatment.
The sector division in the model does also effect the amount of emission emitted during the day and during night, see Table 2.2. The day is defined as 0700-1800 local time, (Simpson et al., 2003). The time factors with acknowledgement to GENEMIS, Generation and Evaluation of Emission, University of Stuttgart (IER) as for the regional EMEP model. Table 2.2 indicated emission from solvent use and other product use, S6, and from road traffic, S7, have 3/4 of the emission output during daytime. These sectors are highly dependent of peoples activities and it is reasonable that there is more traffic during the day. S2, non-industrial combustion plants, S3, combustion in manufacturing industry and S8, other mobile sources and machinery, does also have somewhat higher emission during day. The day/night distribution in emission input is important for processes like chemical reactions where some reactions are dependent of solar radiation.

Sector		0-92m k=20	92-184m k=19	184-324m k=18	324-522m k=17	522-781m k=16	781-1106m k=15
1	Public Power stations	-	-	8 %	46 %	29 %	17 %
2	Com./inst.combustion	50 %	50 %	-	-	-	-
3	Industrial combustion	-	4 %	19 %	41 %	30 %	6 %
4	Production processes	90 %	10 %	-	-	-	-
5	Extraction fossil fuel	90 %	10 %	-	-	-	-
6	Solvents	lowest layer	-	-	-	-	-
7	Road traffic	lowest layer	-	-	-	-	-
8	Other mobile	lowest layer	-	-	-	-	-
9	Waste	10 %	15 %	40 %	35 %	-	-
10	Agriculture	lowest layer	-	-	-	-	-
11	Nature	lowest layer	-	-	-	-	-

Table 2.1: The vertical distribution of anthropogenic emission in each SNAP sector, (Simpson et al., 2003)

Ideally the global model emission should provided the same level of detail as the regional European model. However, this detailed information is not easily available. The factors influenced by sector division is worked out for Europe and is not necessarily the same for the rest of the world. The emission used in the global model are in some cases also more simplified than the emission specified here, see chapter 4.

Sector	1	2	3	4	5	6	7	8	9	10
Day:	1.0	1.2	1.2	1.0	1.0	1.5	1.5	1.2	1.0	1.0
Night:	1.0	0.8	0.8	1.0	1.0	0.5	0.5	0.8	1.0	1.0

Table 2.2: Day and night factors for distribution of anthropogenic emissions in SNAP sectors, (Simpson et al., 2003). Notes: emissions from international shipping assumed constant throughout the day.

Meteorology

The regional model uses meteorological data from PARLAM-PS, in a 3-hourly resolution. PARLAM-PS is a version of the HIRLAM, HIgh Resolution Limited Area Model, Numerical Weather Prediction (NWP) model, with parallel architecture, (Simpson et al., 2003). The global EMEP model applies meteorological input data derived from ECMWF, European Center for Medium range Weather Forecasting. The data is prepared by running IFS, Integrated Forecast System model, with a spectral resolution of T319, (Jonson et al., 2007). The data from IFS is interpolated to long.-lat. coordinates and to the vertical grid in the EMEP model. The interpolation routine contains a Poisson-based filter to secure the mass conservation of the wind fields, (Peter Wind, pers.comm.).
An evaluation of the meteorological driver, the IFS from ECMWF, was presented in Tarrasón et al. (2008), with comparison against meteorological measurements. According to Tarrasón et al. (2008), in general the use of ECMWF meteorological input improves the performance of the EMEP model in Europe for some processes. This is mostly related to the fact ECMWF precipitation fields higher resemblance with observations than PARLAM PS precipitation fields. IFS showed in general reasonable agreement with observed values, for more detailed information on the evaluation of ECMWF meteorology see Tarrasón et al. (2008).

Table 2.3 presents the main meteorological parameters used in the EMEP model. These are, in 3D, wind velocity components - important for both vertical end horizontal advection, humidity, potential temperature, cloud cover and precipitation. For the two dimensional parameters the pressure and temperature are of importance for air density, and dry deposition and stability, as well as surface fluxes and surface stress.

Land-use

Information about land cover is a necessary part in the model, mainly due to the effect on dry deposition modelling and for estimation of biogenic emissions. For each of grid square, the land-use data contains information of the fractional coverage of different vegetation types. The dry deposition module in the EMEP model calculates the resistance in 16 different land-use types. The types are documented in Simpson et al. (2003), and consists of classes like "Temperate/boreal coniferous forests" described with heights, albedo, growing season and LAI-parametes (leaf area index).
In Europe the global EMEP model uses the same land-use as the regional model. For the rest of the world land-use data from MM5, the Fifth-Generation NCAR (National Center for Atmospheric reaserch)/Penn State Mesoscale Model, are applied.
The land-use data from MM5 was interpolated to consists of the 16 land-use types applied in the EMEP model.

Parameter	Unit	Description	Main Purpose
3D fields - for 20 σ levels			
u,v	m/s	Wind velocity components	Advection
q	kg/kg	Specific humidity	Chemical reactions, dry deposition
$\dot{\sigma}$	s^{-1}	Vertical wind in σ coordinated	Vertical advection
θ	K	Potential temperature	Chemical reactions, eddy diffusion
CL	%	Cloud cover	Wet removal, photolysis
PR	mm	Precipitation	Wet and dry deposition
2D fields - for Surface			
P_S	hPa	Surface pressure	Surface air density
T_2	K	Temperature at 2m height	Dry deposition, stability
H	Wm^{-2}	Surface flux of sensible heat	Dry deposition, stability
τ	Mm^{-2}	Surface stress	Dry deposition, stability
LE	Wm^{-2}	Surface flux of latent heat	Dry deposition

Table 2.3: Archived Meteorological Data Used in EMEP Model, (Simpson et al., 2003).

Running the model

The Unified EMEP model is an open source model (*www.emep.int/OpenSource/*). The version available on Internet is however only the regional model, and the global model used in this thesis was made available from Meteorological Institute - met.no Oslo, and EMEP. The model version run is version rv3. Access to the supercomputer in Tromsø, Stallo, was allowed in directions of met.no.

The model was run twice with two different emission inventories for the year 2001, from 01.01.2001 to 01.01.2002. The model results have been compared in a yearly mean and for the months March, July and December. Spin-up time was not included when running the model for a whole year. The assumption that spin-up time is not needed can be justified by the short lifetime of most of the gases, and the fact that the model has initial and boundary conditions that make the spin-up process more reasonable. The lack of spin-up can effect a time period of about a week in the beginning, but it is of minor importance in a yearly perspective studied in this thesis.

Chapter 3

Observational data

Observations of surface concentrations from EANET, are used as basis for the evaluation of the global EMEP model results in Asia. The EANET network started up in March 1998 in Yokohama in Japan. The network was established as a regional cooperative initiative to promote efforts for environmental sustainability and protection of human health in the East Asian region. The initiative for the monitoring network, was a recognition that the rapid industrialization in the area that could cause dangerous effects for the environment and in particular acid rain.
EANET's monitoring activities became a reality on a regular basis from January 2001, with the participation of 10 countries, namely China, Indonesia, Japan, Malaysia, Mongolia, Philippines, Republic of Korea, Russia, Thailand, and Vietnam. Later Cambodia, Laos PDR and Myanmar joined EANET in 2001, 2002 and 2005, respectively. There are currently 13 countries participating in EANET activities, (Acid Deposition and Monitoring Network in East Asia, 2009).

The observations from EANET used in this thesis where made available trough NILU. The data was compiled by NILU and CCC under work for the Task Force on Hemispheric Transport of Air Pollution.

3.1 The EANET network

The EANET monitoring sites are classified in two categories: (1) an acid deposition monitoring site, (2) an ecological survey site. Ecological survey sites are for soil and vegetation monitoring and inland aguatic monitoring.
In this thesis the acid deposition monitoring sites are used. Under this category the observation is of wet deposition and dry deposition (started as air concentration). Wet and dry deposition was monitored in order to observe concentrations and evaluate fluxes of acidic substances deposited to the land surface (Network Center for EANET, 2002). The components measured in air concentration with instrumental measurements were SO_2, NO_2, NO, O_3 and PM. The impact of acid deposition formed a threat to the ecosystems and the monitoring assessed important information of the state of acid deposition in Asia. Later the impact on health aspect also became a subject of interest and different particle components where monitored.

The acid deposition monitoring site are classified in three sub-categories; urban, rural or remote sites. These sub-categories are identified according to the distance from the site to large pollution sources, as cities or local industrial plants.

An **urban** site is situated in urbanized and industrial areas, and also in areas immediately out-

side urban areas. The data from this site can for instant be used to evaluate the effects of acid deposition on buildings and historical monuments or human health.

A **rural** site must be more than 20 kilometers away from large pollution sources like cities, power plants, or highways. The data can be used for evaluation of acid deposition on agricultural crops, forests, etc.

Remote stations must be located more than 50 kilometers away from large pollution sources like cities, power plants, or highways. It has to be more than 500 meters away from main roads, which are defined as roads with more than 500 vehicles per day. These data are often used to evaluate long-range transport and deposition models.

3.1.1 Sites in year 2001

The observations used in this thesis are from 2001. In this year 43 acid deposition monitoring sites where located in a large area in East Asia. The area is confined between 51 ° North to 6 ° South.
In Figure 3.1 the EANET sites are placed on a simple map over East Asia. The map visualizes EANET monitoring sites throughout East Asia in the year 2001 (Network Center for EANET, 2002).

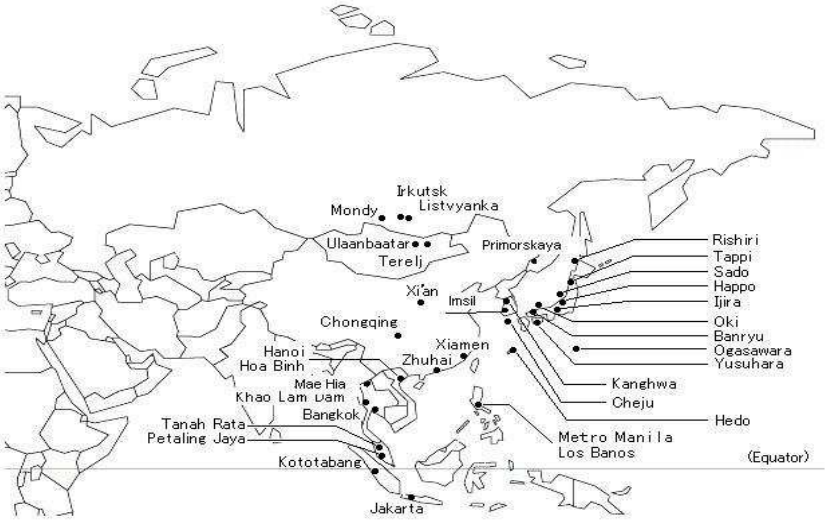

Figure 3.1: Locations of EANET sites 2001, (Network Center for EANET, 2002). Note that "Xiàn" includes three sites, while "Chongqing", "Xiamen" and ""Zhuhai" all includes two sites.

The 43 sites includes 15 urban, 12 rural and 16 remote sites (Network Center for EANET, 2002). Note that even though there are 43 sites, not all have observation of for instance dry and wet deposition of NO_x, SO_2 or O_3.

3.1.2 Sites used for comparison in this thesis

The sites used for comparison in this thesis for 2001 are listed in Table 3.1. 16 sites are presented, 5 urban, 3 rural and 8 remote. Most of the sites are situated in Japan, but there were also information available for 3 sites in China and two in Thailand.

Country	Number	Name of site	Area	Lat.	Long.	Meters over sea level
China	2	Jinyunshan (Chongqing)	Rural	29 °49'N	106 °22'E	800m
	4	Weishuiyuan (Xiàn)	Rural	34 °22'N	108 °57'E	360m
	6	Hongwen (Xiamen)	Urban	24 °28'N	118 °08'E	50m
	8	Xiang-Zhou (Zhuhai)	Urban	23 °16'N	113 °31'E	-
Japan	14	Rishiri	Remote	24 °28'N	118 °08'E	40m
	15	Tappi	Remote	41 °15'N	141 °21'E	105m
	16	Ogasawara	Remote	27 °05'N	142 °13'E	320m
	17	Sado	Remote	38 °14'N	138 °24'E	110m
	18	Happo	Remote	36 °41'N	137 °48'E	1850m
	19	Oki	Remote	36 °17'N	133 °11'E	90m
	20	Yusuhara	Remote	33 °22'N	132 °56'E	-m
	21	Hedo	Remote	26 °09'N	128 °03'E	60m
	22	Ijira	Rural	35 °34'N	136 °42'E	140m
	23	Banryu	Urban	34 °04'N	131 °42'E	60m
Thailand	37	Bangkok	Urban	13 °46'N	100 °32'E	2m
	38	Samutprakarn (Bangkok)	Urban	13 °44'N	100 °34'E	2m

Table 3.1: Information on EANET sites used in this thesis.

Spatial representativeness

The sites are mostly allocated in Japan, and to a less degree they represents areas in China and Thailand. China is the country in Asia that covers the greatest area and contributes a great deal to air pollution. The scarce selection of locations in Asia can give a poor basis of comparison. It is not optimal that there are so few stations for validation in the main continent, but unfortunately no data was available for other sites for the year 2001.

In addition to the scarce observation data, another effect is significant when comparing model results and observations concerning the representativeness of the data. The model results are given in mean grid box values, with horizontal grid resolution of 1° x 1° used in the global EMEP model. The grid box is an area of a substantial size and can contain large pollution sources and also remote land areas. Therefore, by averaging each grid box over this coarse resolution it can give concentrations not representative for the specific site of comparison.

Temporal representativeness

The observations from EANET where made available trough NILU. The data from Japan and Thailand were hourly concentrations, while the measurements from China were given in daily concentrations. The observational data was processed by using a fortran program made available

by EMEP, for accumulating the hourly data into daily averages. For this thesis a modification was included, here only considering daily data with more than six hours of observations.

Units

The observations were presented in parts per billion, ppb. The EMEP model calculates the results for SO_2 and NO_2 in $\mu Sg/m^2$ and $\mu Ng/m^2$, respectively. The observational data was converted to the same units for comparison. An assumption of pressure of 1013 hPa and temperature of $20\,^\circ$ C was made for most of the sites. SO_2 values where multiplied with 1.330 and NO_2 where multiplied with 0.582.
The exception was the mountain station Happo, situated at 1850 meters height. Here it is assumed pressure of 800 hPa and temperature of $0\,^\circ$ C, this calculated for the SO_2 values to be multiplied with 1.128 and NO_2 multiplied with 0.493.
There was no conversion of O_3 units.

Plotting

Timeseries where plotted by a program med available by met.no. In the figures constructed daily values are plotted. Some days and months had scarce data, here no line will appear.

Chapter 4

Emission data

Emission data is an essential part in any chemical transport model. Knowledge about emissions is important for the model results and understanding of air pollution. The first preliminary evaluation of the global EMEP model, (Jonson et al., 2007), showed the model to underestimate air concentrations at ground level of SO_2 and NO_2 in Asia. The further recommendations were that the emission data and measurement data over Asia should be revised.
This chapter contains an analysis of the emissions originally used in the global EMEP model. Problems with the emission data are identified, in particular with respect to sector data allocation over Asia.
The original emission data in the global EMEP model is compared with a different emission inventory over Asia. The inventories differs for SO_2, NO_2, CO and NMVOC, where both are based on emission data from ACESS. The two emission inventories are evaluated with each other, and against other estimates from scientific literature for different continents and in particular Asia. The main difference between the emissions inventories is the source sector distribution. The emission input originally in the global EMEP model, is called ***Original*** throughout the thesis, and the new input data, is called ***ACESS***.

4.1 *Original* global emissions in EMEP

The emission input used in the global EMEP originally was a compilation from different sources. These are documented in Jonson et al. (2007): in the Southern Hemisphere and over North America, the global emissions was adapted from the OsloCTM2 emission input. In the EMEP area, European emissions was used, to secure that the results from the global model over Europe was as similar as possible to the results from the regional EMEP model. Over Asia, the OsloCTM2 emissions was replaced by a bottom up inventory developed for East Asia for the year 2000 (Streets et al., 2003) available through ACESS.

The EMEP model uses emission input data of SO_x, NO_x, NH_3, NMVOC, CO and PM. And the understanding of the sources for the emission is highly relevant when analysing the emission estimates. The main sources of the global emission are given from different scientific literature and presented in section 4.1.3. The main sources of the emission in Asia in particular are given in section 4.4.1. The pollutants discussed in these sections are mainly SO_x, NO_x, CO and NMVOC, since these are the gases that differs in the two emission inventories.

4.1.1 Global emission totals

In order to review the validity of the emission estimates in the *Original* emission data set, the totals from the input data in the global EMEP model have been compared with other independent estimates of emission totals around 2001. The estimates are presented as follows.

The first estimates are from IPCC, Intergovernmental Panel on Climate Change, and the report IPCC Special Report on Emissions Scenarios, (Nakicenovic et al., 2000). The report has estimates from multiple models and the numbers from the year 2000 are the baseline used for different emission predictions.

The second estimates are from Cofala et al. (2007). Here a global version of the Regional Air Pollution Information and Simulation, RAINS model was used to estimate anthropogenic emissions for the period 1990-2030. The analysis did not include emissions from international shipping, aviation, open biomass burning and natural emissions.

The third emission estimate are from EDGAR, Emission Database for Global Atmospheric Research, National Institute of Public Health and the Environment. The estimate is used for comparison in the article by Cofala et al. (2007). The EDGAR information system stores global emission inventories of greenhouse gases and air pollutants from anthropogenic sources including halocarbons and aerosols both on a per country and region basis as well as on a grid, (EDGAR, 2005).

The forth estimates are from Earthtrends, WRI, World Resources Institute. The numbers are retrieved via Internet (available at $http://earthtrends.wri.org/$), and the sources are described as "The Netherlands National Institute for Public Health and the Environment/The Netherlands Environmental Assessment Agency (RIVM/MNP) and the Netherlands Organization for Applied Scientific Research (TNO)", (World Resources Institute, 2007).

The fifth estimate are from Seinfeld J.H. and Pandis S.N. (1998). The estimates of total global emission are calculated for the decade before 1998. These estimates are therefore from earlier years, and the development in the emissions must be taken under consideration when interpreting the results.

	Original EMEP (2001)	IPCC (2000)	Cofala (2000)	EDGAR (2000)	WRI (2000)	Seinfeld and Pandis (Decade before)
SO_2	97 (SO_x)	65-75	96	138	150	~80
NO_x	126	30-33	83	90	127	~52
CO	911	800-900	542	531	1 077	
NMVOC	121	130-150			186	~142

Table 4.1: Different global emission estimates of SO_2, NO_2, CO and NMVOC in years around 2001 [Tg/year].

Table 4.1 presents the global emission estimates in the *Original* EMEP emission data compared with the different emission estimates described above. It should be noted that the *Original* global EMEP emission estimates in this table are not the same as the tables given in EMEP Technical Report 2/2007, (Jonson et al., 2007), because there the values does not include the EMEP-area.

The emission data in Table 4.1 includes the whole global domain.

The estimates of SO_x global emission are of different sizes, from 65 Tg/yr in IPCC to around 150 Tg/yr in the WRI estimate. EDGAR also has a high estimate of 138 Tg/yr, the high estimates in EDGAR is according to Cofala et al. (2007) most likely caused by omission of emission control measurements started after 1990 and also possibly the reason for IPCC high prediction of SO_2 emission.
Another estimate of global SO_2 emission is found in Smith et al. (2004), which gave a global estimate of ~60-70 Tg/yr SO_2 emission in 2000. The global EMEP *Original* emissions of SO_2 are within the range expected to be reasonable, considering that different emission sources can be included.

NO_x estimates from the *Original* EMEP and WRI are in excellent agreement. The other estimate are in a lower range. Not knowing the details in the calculations of the estimates makes an suggestion that for IPCC and EDGAR, it is possible that some of the models for instance did not include energy-related sources. The estimate from Cofala did not include emissions from international shipping and aviation reflecting the low emission total. Seinfeld and Pandis have calculations of the global emission estimate from the decade before and is expected to be lower. The *Original* EMEP emission totals for NO_x are assumed to be reasonable.

CO shows good agreement in the estimates with emission totals around 900 Tg/yr, except for the low estimates found in Cofala and EDGAR, which are most likely due to the exclusion of emissions from international shipping and aviation. The emissions estimates of CO and NMVOC have a great deal of uncertainties and especially for some regions, due to variety in emission sources and dependency of factor difficult to measure. Emission of NMVOC is to some extent lower in the *Original* EMEP, however, multiple factors can be effective and the estimate are assumed to be reasonable.

Concluding from the comparison of global emission estimates in Table 4.1 that the *Original* EMEP is in good agreement with other global emission estimates. The totals in the *Original* emission inventory are therefore considered to be reasonable.

4.1.2 Emission distribution in continents

The yearly emission totals in the *Original* emission data is further analysed by investigating the values of emissions in different continents of the world. A division into six areas corresponding to the different continents are visualized in Figure 4.1 and are given as followed:
Asia is extending from latitude 13 °S to 60 °N, and longitude 53 °E to 157 °E.
Europe from latitude 35 °N to 90 °N, and longitude 20 °W to 53 °E.
Africa from latitude 60 °S to 35 °N, longitude 20 °W to 53 °E.
Oceania from latitude 60 °S to 13 °S, longitude 53 °E to 180 °E.
North-America from latitude 10 °N to 90 ° N, longitude 20 °W to 160 ° W.
South-America latitude 60 °S to 10 °N, longitude 20 °W to 160 °W.
A term called RoW represent Rest of the World and is the area not included in the squared regions visualized in the map. This area contains a small part of the total emission estimate since the area includes few high emission sources, and are not discussed in further analyses.

The estimates of the *Original* emissions in the continents are given in Table 4.2 for the four pollutants with units of Tg/yr. Asia is the main single emitter of SO_x emissions, with 41.64 Tg

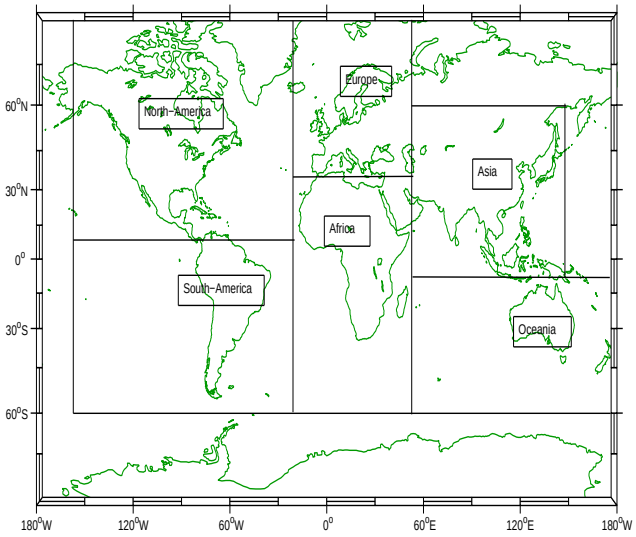

Figure 4.1: The division in continents used for analysis of emission data.

	Africa	Asia	North-America	South-America	Oceania	Europe	RoW	Total
SO_x	4.88	41.64	16.77	5.96	1.66	24.53	1.24	96.68
NO_x	23.21	28.49	29.97	13.79	8.84	21.44	0.55	126.29
CO	215.50	242.55	148.36	145.73	83.53	61.68	13.84	911.19
NMVOC	19.73	43.13	12.23	22.37	6.15	16.77	1.46	121.84

Table 4.2: *Original* emission estimates of SO_x, NO_x, CO and NMVOC distributed by continents for 2001 [Tg/year].

pr year. Asian emissions in 2000 are almost twice as high as European emission the same year, with 24.53 Tg pr year. In the introduction emission estimates for Asia from Ohara et al. (2007) were presented, with estimates of SO_2 calculated to 41.49 Tg/yr for 2000. This estimate is in agreement with the *Original* emission input for the area.
In Figure 4.1 Europe is a small extension of the EMEP-area, which has been validated in the regional model over several years and is assumed to be reasonable. The EMEP emissions are provided by Parties of the CLRTAP Convention. The estimates in the *Original* inventory correspond well with EDGAR emissions, which in 1995 estimated 27 Tg/yr, and therefore in agreement with the known decrease in European emissions since 1995. However it is not clear how independent EDGAR and EMEP estimates are over Europe.
Africa, South-America and Oceania have significantly lower estimates, at around 5 Tg/yr or less. The industrialization of the three continents has not experienced the same rapid development and high levels as Asia or North-America.

North-America, Asia, Europe and Africa have all high emission estimates of NO_x, and North-America has the highest estimate. Automobiles are main emitters of NO_x emission, which makes the high emission in North-America, Europe and Asia reasonable. An estimate of North-

America emission of NO_x in 1995 show emission totals of 25 Tg/yr, with the value derived from EDGAR Emission Database (Cooper and Parrish, 2004). Considering the possible increase in emission from 1995 to 2000, the estimates for North-America are reasonable in the *Original* emission inventory.
The high contribution from Africa is further analysed. Cofala et al. (2007) estimates NO_x emission in "Africa and Latin America" in 2000 to be 15 Tg/yr. These estimates are lower then the *Original* emission estimate, and includes Latin America as well. Therefore an estimate from WRI in the year 2000 for Africa and the Middle East is included, with value of NO_x emission of 22.5 Tg/yr which are in good agreement with the *Original* emission estimate for Africa considering parts of the Middle East are included in the region. The estimates for the *Original* EMEP are considered to be reasonable.

CO and NMVOC have both highest emission estimates from Asia. The estimates from Ohara et al. (2007), had CO emissions of 305 Tg/yr and NMVOC emissions of 40 Tg/yr for 2000, while the *Original* emission inventory show lower values for CO emission. A detailed comparison of the Asian emission estimates are given in section 4.3. As mentioned earlier, are the estimates of CO and NMVOC associated with high uncertainties and the estimates can include or exclude different emission sources. Comparison with the other continents emission estimates are not conducted in particular since recent available literature is scarce.

For further analysis of the *Original* emission inventory used in the global EMEP model, the distribution in the source sectors are analysed.

4.1.3 Emission distribution by sectors

The EMEP model distributes the emission data into SNAP sectors according to the emission sources, see chapter 2.1 for description of the 11 sectors in the model. By dividing the emissions into sectors the model shows a better validation of the actual sources. Knowledge about the activities responsible for the emissions, is relevant for understanding the model results and effects in the atmosphere. The division into sectors gives a more detailed distribution of the emissions in a temporal and spatial sense.
The *Original* emission data is analysed here by quantifying the sector distribution for NO_x, SO_2, CO and NMVOC. Figure 4.2 visualizes the emission estimates in each sectors, where the emissions are given in Tg/yr and the continents cover the same area as in the previous subsection.

The four pollutants analysed are emitted from various sources, and to validate the sector distribution in the *Original* emission inventory, the main global emission sources for the different pollutants are presented below.

According to Cofala et al. (2007), is the power section, with more than 50%, the largest emitter of global anthropogenic SO_2 emissions in 2000, and about 1/3 comes from industry. Note that these estimations are for global anthropogenic emissions and it is important to remember that the percentage can vary in different places, and this is valid for all pollutants. Another global estimate is given by TEMIS, Tropospheric Emission Monitoring Service in the Netherlands. Here SO_2 are considered to have coal burning as the single largest man-made source, accounts for about 50% of annual global emissions. The next largest source of SO_2 emissions is oil burning accounting for a further 25 to 30 percent, (Tropospheric Emission Monitoring Internet Service The Netherlands, 2009). Fossil fuel, coal, oil and gas provide electric power and energy. Fossil fuel provide around 66 % of the world's electrical power, and 95% of the world's total energy

demands and here heating, transport, electricity generation and other uses are included, (ENERG UK, 2009). This indicates the importance of S1, combustion of energy and transformation industries. S3, combustion in manufacturing industries, is also one of the main source activities for SO_2.

According to Jacob (1999), does combustion of fossil fuel account for about half of the global source of NO_x. Fossil fuel are mainly coal, oil and gas, which are formed from the fossilised remains of prehistoric plants and animals. The concentration of NO_x in the exhaust gas is decided by the combustion conditions, like temperature and air-to fuel ratio (Nakicenovic et al., 2000). Especially road transport and ships emits high concentrations of NO_x with their internal combustion engines. However fossil fuel are also used in providing electric power and energy. S7, road transport, and S8, other mobile sources and machinery are important sources of NO_x as well as S1, combustion in energy and transformation industries.

Sources like technological processes, combustion and industrial processes and biomass burning are major sources for emission of CO according to Jacob (1999). This is in agreement with Cofala et al. (2007) suggestion that about half of anthropogenic CO emissions originates from the residential/commercial sector, and one-third from road transport. Third and fourth largest emission sources are industry and non-road vehicles, contributing with 8% and 6% to CO emission, respectively. The main SNAP sectors are therefore S2, non-industrial combustion plants, and S7, road transport. Contribution from S3, combustion in manufacturing industries, and S8, other mobile sources and machinery, are also of importance according to Cofala et al. (2007).

VOC denotes the entire set of vapor-phase atmospheric organics, excluding CO and CO_2, and NMVOC excludes also methane. According to Seinfeld J.H. and Pandis S.N. (1998) the highest contribution of NMVOC in 1987, measured by Southern California Air Quality Study, were road transport. Thereafter follows other fuel consumptions like wood, solvent use and crop residues, here including waste. For Asia, with detailed analysis in section 4.4.1, Streets et al. (2003) calculated that emissions were largest from the residential combustion of coal and biofuel, about 34%, and from transportation, 27%. In United States Seinfeld J.H. and Pandis S.N. (1998), suggested the contribution to be highest from motor vehicles. In SNAP sectors the main sources are thus S7 and S8, road transport, and other mobile sources and machinery. Also S2, non-industrial combustion plants, and S6, solvent use and other product use, are of some importance for CO emission.

Figure 4.2 provides an overview of the four pollutants and their continental distribution in sectors. The RoW-term is excluded here.
As it can be seen from Figure 4.2, Asia has a similar sector distribution for all pollutants, where S7, road transport, has the highest contribution.
The main source activities of each gas was presented above, and the sector distribution in the *Original* emission input is not in agreement with this description. It appears that the *Original* emission data used in the global EMEP model for Asia has been divided into only two source groups; 'large point source' and 'area sources'. These emissions were placed in two EMEP sectors when implemented in the *Original* EMEP emission input; S1, combustion in energy and transformation industries and S7, road transport. The assumption was that 'large point source' were distributed in S1, and 'area sources' in S7. This implies separating only a high and a low source, with S1 being emitted at higher altitudes than S7, which were emitted in the lowest layer. Note that also the other pollutants in the emission input data for the global EMEP model; NH_3

and PM, show the same sector distribution in Asia in the *Original* emission inventory as the pollutants discussed here. The *Original* emission data for Asia is therefore an oversimplification of the actual sector distribution of the emissions.

Figure 4.2 also indicates an error in the sector distribution in other continents. A substantial amount of emission is distributed in S10, agriculture, and S11, other sources and sinks, in other continents than Asia and Europe. The implication of this error will not be discussed in this thesis since it is outside Asia. However the global EMEP emission input are recommended to be investigated closer for applications outside Asia.

4.2 *ACESS* emissions in Asia

The *ACESS* emission input is from an inventory developed for Asia by Qiang Zhang and David G. Streets, from the Argonne National Laboratory. It was produced for the INTEX-B (The Intercontinental Chemical Transport Experiment - Phase B) a project of the National Aeronautics and Space Administration (NASA), (Streets and Zhang, 2008). The domain for the emission input is shown in Figure 4.3. The emission data is available at the ACESS web-page ($http://www.cgrer.uiowa.edu/EMISSION\_DATA\_new/index\_16.html$. The emission files available includes SO_2, NO_x, CO, NMVOC, PM10, PM2.5, BC, and OC, and VOC. They are four files for every sector; power, industry, residential, and transportation, and for VOC six speciated sector files are provided.

The emission data for SO_2, NO_x, CO, NMVOC was implemented in the global EMEP model emission data for Asia and the new inventory is called *ACESS*. However it is important to note that the source sector definition used by ACESS is different then the SNAP sector definitions used in the EMEP model.
In the following will the implementation of the files be described. Thereafter a comparison of different estimates of emission totals in Asia. And further a presentation of the *ACESS* emission data compared to the *Original* emission data is given for Asia, with special interest in the sector distribution.

4.2.1 Implementation of ACESS emissions in the global EMEP model

Sector distribution

The sector distribution in ACESS includes four sectors; Industry, Transportation, Power and Residental. The sector division in ACESS were not further explained. And for the SNAP sectors used in the EMEP model there is broader classifications of the activity sectors. However the four sectors were compared with the 11 SNAP sectors used in the EMEP model, and the following correspondence was established.
Power = S1 (Combustion in energy and transformation industries)
Industry = S3 (Combustion in manufacturing industries)
Residental = S2 (Non-industrial combustion plants)
Transportation = S7 (Road transport) + S8 (Other mobile sources and machinery)

Transportation can be distributed in both S7, road transport, and S8, other mobile sources and machinery. However an simplification was made and S7, road traffic, is assumed to have a higher

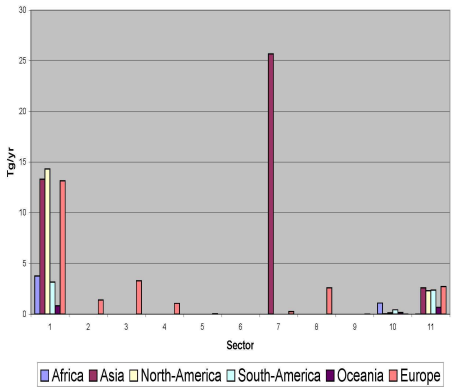

(a) SO_2

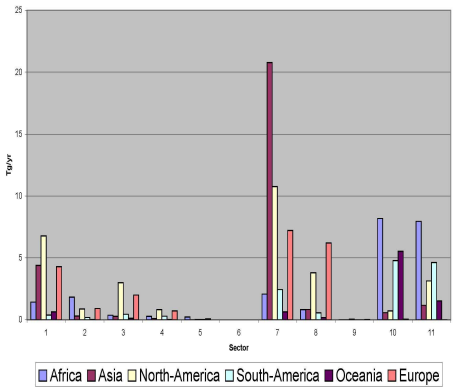

(b) NO_x

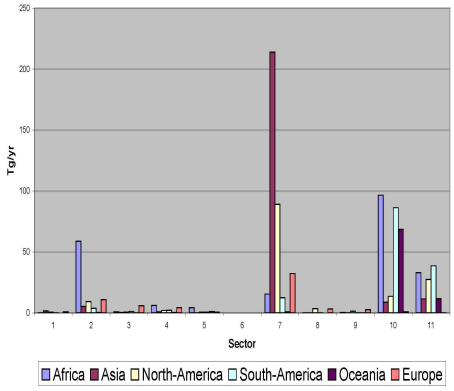

(c) CO

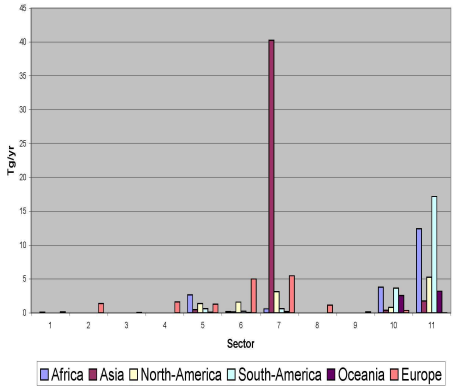

(d) NMVOC

Figure 4.2: Estimates of the *Original* emissions of SO_2, NO_2, CO and NMVOC for 2001 in different continents [Tg/yr].

contribution. Therefore the emission from Transportation is distributed in S7. This simplification gives no difference in height distribution, however there is more emitted during day in S7, road transport, than S8, other mobile sources and machinery.

Emission year

The ACESS emission inventory are available with emission data for the year 2006 at the ACESS webpage. In this thesis the year for the emission input used for Asia were 2000, so the emission

Figure 4.3: ACESS domain, (Streets and Zhang, 2008)

data had to be adjusted to an earlier year. At the ACESS web-page a table summarizing the changes from the ACESS (TRACE-P Modelign and Support Systyem) 2000 emission to ACESS (INTEX-B) 2006 emissions. The table on the web-page shows percentage change derived in the different sectors for BC, OC, SO_2, NO_x, CO and NMVOC. Of these pollutants, SO_2, NO_x, CO and NMVOC are used in the EMEP model input data, and the changes for these gases, from 2000 to 2006, are shown in Table 4.3.
It is important to note that the changes can be caused by not only growth in emissions, but also effects of replacing the TRACE-P inventory (2000) by local inventories in several countries, and possible improvements made to the original TRACE-P inventory (2000) Streets and Zhang (2008). However without knowledge about the percentage amount of these effects, the changes are here taken as increase in emissions. The adjustment factors are given for Asia as a total.

	Power	Industry	Residental	Transport	Total
SO_x	56,9%	43,0%	7,6%	-3,7%	43,4%
NO_x	90,7%	72,8%	22,6%	40,3%	61,8%
CO	N/A	204,2%	17,2%	8,7%	41,4%
NMVOC	541,2%	70,2%	18,0%	29,7%	35,7%

Table 4.3: Percentage change of emissions in Asia from ACESS 2000 to ACESS 2006 in different source sector, (Streets and Zhang, 2008). Note N/A = high number.

Components

The EMEP model uses emission input data consisting of SO_2, NO_x, NH_3, NMVOC, CO, $PM_{2.5}$ and PM_{10}. The pollutants replaced in the *Original* emission inventory was SO_2, NO_x, NMVOC and CO, then called the *ACESS* emission inventory. Note that the two emission inventories does not differ for the emissions for the remaining pollutants; NH_3, $PM_{2.5}$ and PM_{10}. The reason for not replacing these pollutants are related to the fact that no increase were presented from the ACESS 2000 to ACESS 2006 for NH_3 and PM at the web-page.

Temporal variation

The emission files provided by ACESS were given in yearly data. In this report there is not implemented any seasonal variation in the emission input. The emission data were divided in twelve equal emission totals and distributed in monthly files.

Grid resolution

The global EMEP model has a grid resolution of 1° x 1° for the input data. While the *ACESS* inventory has a 0.5° x 0.5° resolution. The values from ACESS were then extrapolated in a 1° x 1° grid and became in the same manner as the global EMEP model.

Data processing

A new fortran program was developed for reading the files downloaded from the ACESS web-page. The program involved also grid size extrapolation, sector division, adjustment to year and preparation of monthly input. The emissions of NO_x, SO_2, CO and NMVOC were replaced in the *Original* global EMEP emission input files, creating a new inventory: the *ACESS* emission inventory. The emissions of NH_3, $PM_{2.5}$ and PM_{10} were not replaced and are the same in both emission inventories. NMVOC is called VOC on the web-page, however after consulting with Qiang Zhang in ACESS it became clear that VOC are NMVOC, without methane.

4.3 Evaluation of emission totals in Asia

In order to validate the emission totals, both in the *Original* and in the *ACESS* emission input data, a comparison with other estimates available in scientific literature was carried out. The comparison is summarized in Table 4.4. The different peer reviewed estimates are presented here:

The first estimate is from Streets et al. (2003). This is an inventory of gaseous and primary aerosol emissions in Asia in the year 2000. The inventory was developed to support atmospheric modeling and analysis of observations taken during the TRACE-P experiment funded by the National Aeronautics and Space Administration (NASA) and the ACE-Asia experiment funded by he National Science Foundation (NSF) and the National Oceanic and Atmospheric Administration (NOAA). Emissions were estimated for all major anthropogenic sources, in 64 regions of Asia.
This inventory is not independent of ACESS, and therefore also the *Original* and the *ACESS* emissions inventory.

The second estimate is from Cofala et al. (2007). Here a global version of the Regional Air Pollution Information and Simulation (RAINS) model and its GAINS extension to greenhouse gases was used. There were prepared estimates of anthropogenic emissions for the period 1990-2030 for 75 countries or country groups. The analysis did not include emissions from international shipping, aviation, open biomass burning and natural emissions.

The third emission estimate are from EDGAR, Emission Database for Global Atmospheric Research, National Institute of Public Health and the Environment. The estimate is used for comparison in the article by Cofala et al. (2007). The EDGAR information system stores global

emission inventories of greenhouse gases and air pollutants from anthropogenic sources including halocarbons and aerosols both on a per country and region basis as well as on a grid, (EDGAR, 2005).

The fourth estimate is from Ohara et al. (2007). They developed an emission inventory for Asia, REgional Emission inventory in ASia (REAS), for the period 1980-2020. The inventory included NO_x, SO_2, CO, BC, OC, CO_2, N_2O, NH_3, CH_4 and NMVOC from anthropogenic activities. Open biomass burning were not included. The emissions from international shipping and international aviation are also excluded. Note that these estimates are not independent of Streets et al. (2003), for instance NMVOC emissions were obtained from Streets et al. (2003), and allocation factors for road networks and rural populations were provided by Streets et al. (2003).

The different estimates are given in Table 4.4, here the two first estimates are from global EMEP inventories, the *Original* and the new implemented *ACESS* inventory, respectively. The two emission estimates in the *Original* and the *ACESS* are in agreement. This is related to the adjustment of the emissions from ACESS 2006 to 2000 given on the basis of the emissions from TRACE-P used in the *Original* emissions.

	Original EMEP 2000	*ACESS* EMEP 2000	Streets et al. 2000	Cofala et al. 2000	EDGAR 2000	Ohara et al. 2000
SO_2	41.64	42.46	34.30	32.00	54.00	41.25
NO_x	28.49	28.71	26.80	22.00	28.00	25.11
CO	242.55	243.66	279.00	236.00	221.00	305.42
NMVOC	43.13	43.43	52.20			40.24

Table 4.4: Different emission estimates in Asia for SO_2, NO_2, CO and NMVOC [Tg/year].

Both the *Original* and the *ACESS* emission input data for Asia are in good agreement with the peer-reviewed other estimates. Note that the emission estimates from EMEP, the *Original* and the *ACESS*, included the area for Asia shown in Figure 4.1, where Asia is extending from latitude 13 °S to 60 °N, and longitude 53 °E to 157 °E. The areas from the other estimates are not necessarily of the same size. For instance Streets et al. (2003), used a domain that stretches from Pakistan in the West to Japan in the East, and from Indonesia in the South to Mongolia in the North. This areas consist of a smaller domain than the *Original* and the *ACESS* emission estimates. This must be considered when comparing the estimates.
Note that there are also differences in including international shipping in the estimates. This is not included in Cofala et al. (2007), however in Streets et al. (2003), Ohara et al. (2007) and both the global EMEP emission estimates include international shipping lanes.

The estimate from EDGAR for SO_2 have higher emissions than the other and even higher than the value for 2006 from ACESS. Cofala et al. (2007) suggested the reason to be that EDGAR omitted the account of emission control measures that was put in operation in 1990. The other estimates for SO_2, accounting for the differences in area included, does not differ significantly from each other.

NO_x is in good agreement for the different estimates, however the inclusion or exclusion of

international shipping and aviation can contribute to differences. A comparison done by Ohara et al. (2007), where estimates without the emissions from shipping and aviation showed that the TRACE-P or Streets et al. (2003) values, were smaller then RAINS (Ohara et al., 2007), and EDGAR had higher emission values. Considering that international shipping and aviation are included for Streets et al. (2003), and the *Original* and the *ACESS* emission inventories in Table 4.4, the conclusions made in Ohara et al. (2007) are reasonable. However the estimate from Cofala et al. (2007) is the lowest estimate, here shipping and aviation is excluded, but the values are still to an extent lower than EDGAR and Ohara et al. (2007). The comparison of NO_x emission estimates in Table 4.4 can indicate a lower estimate in the global EMEP estimates, Streets et al. (2003) and Ohara et al. (2007), but the estimates are not significantly different and the *Original* and the *ACESS* emission estimates are therefore assumed to be reasonable.

CO and NMVOC have variable estimates, which reflects the difficulties and uncertainties in the evaluation of the emission of these species. Ohara et al. (2007) has estimates over 300 Tg/yr for CO emission, significantly higher than the other estimates for 2000. According to Ohara et al. (2007) this difference is related to the applications of higher emission factors for coal combustion. For NMVOC the basis of comparison is less, however the number presented are of the same magnitude, except for high estimates of NMVOC in Streets et al. (2003).

The evaluation of the emission totals for Asia in Table 4.4 indicates that the totals in the *Original* and the *ACESS* emission data are reasonable. Further analysis of the emissions and their sector distribution in the two emission inventories are conducted.

4.4 Main differences in emissions in Asia

The main differences between the *Original* and the *ACESS* emission input are described in this section. The differences related to the sector distribution are discussed first. Then the spatial distribution of the two emission inventories are visualized, and the intensities and high source regions are identified. The differences in spatial distribution of the totals for the two emission inputs, and the differences in spatial distribution in sectors are presented. The emission totals are visualized in percentage and emission differences for the sectors. Finally, an initial analysis of how the differences in the emission inventories are expected to affect the model results are presented.

4.4.1 Differences by sector distribution in Asia

In this section the differences between the *Original* and the *ACESS* emission input data in source sector distribution are analysed. Figure 4.4 visualizes the differences for the different pollutants. The emissions are given in Tg/year and the area reviewed is the squared Asia in Figure 4.1.

Figure 4.4 shows the main differences in sector distribution for all gases. As indicated earlier in this chapter the new inventory *ACESS* has a lower contribution in S7, road transport, then in the *Original* emission input for all pollutants. The distribution in the *Original* emission data was an oversimplification and provided too high values in S7, road transport.
The new distribution made in the *ACESS* emission input involve more sectors: S1, combustion in energy and transformation industry, S2, non-industrial combustion plants, S3, combustion in manufacturing industry, and S7, road transport.

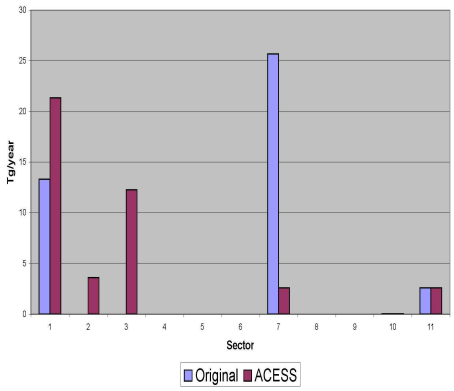

(a) SO_2

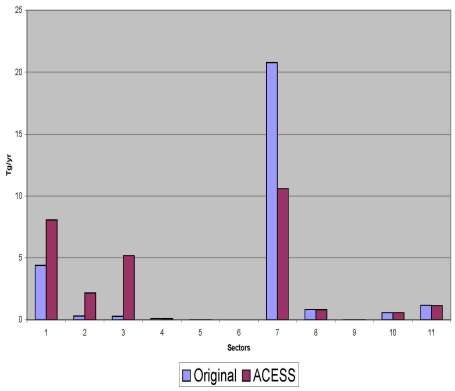

(b) NO_x

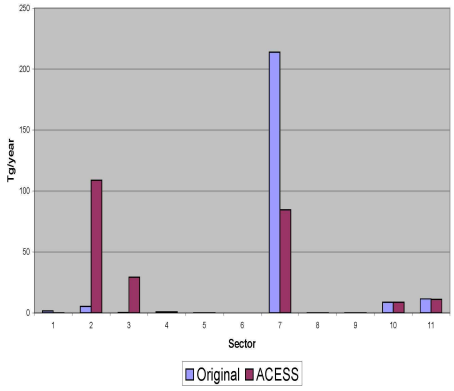

(c) CO

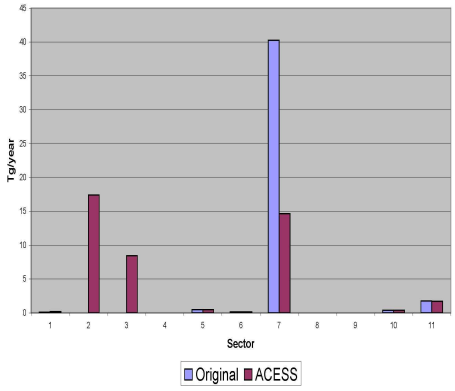

(d) NMVOC

Figure 4.4: The *Original* vs the *ACESS* emission sector distribution as used in the EMEP model in Asia 2000

The four pollutants analysed are emitted from various sources, and a validation of the sector distribution in Asia in particular are presented. The main sectors for the pollutants analysed are described below.

According to Streets et al. (2003), SO_2 is the pollutant best known of the emission contributors in Asia. The reason for this understanding was the concern of the high concentration of this pollutant in cities and that the area was threaten by acid rain. Japanese researchers studied

emission if SO_2 for more than 10 years ago.
Streets et al. (2003) suggested that 45% of production of SO_2 was accounted to the power generation sector, here mainly by the Chinese coal-fired power plants. Secondly the industrial sector stands for 36 %. Ohara et al. (2007) has a distribution of SO_2 emission in Asia 2000 where power plants are the largest source, 35 %. Also here is industry the second largest emission source, with 28%, after this comes domestic and transport sources. The *ACESS* sector distribution is in better agreement with the peer reviewed estimates.

NO_x has according to Streets et al. (2003), the largest source in transportation, 37%. After the main source follows power generation, with a contribution of 27% and industry, with 18 %. The *ACESS* emissions has highest input in S7, road transport, thereafter S1, combustion in energy and transformation industries, and S3, combustion in manufacturing industries. According to Ohara et al. (2007), the NO_x emission in Asia in 2000 have the highest contribution from transport oil use, with 34 %. Second comes power plants, with 22%, and third industrial coal use, with 14%. The percentage distribution is not identical for the two estimates, but the main and second source are the same. This is also in agreement with the *ACESS* inventory, seen in Figure 4.4.

Estimates of CO has a great deal of uncertainties, where the emission depend on the efficiency in the combustion processes and how the equipment is maintained and operated. Streets et al. (2003) suggest an source distribution in Asia for 2000 where 34% comes from residental biofuel combustion and 28% from transportation. There is also a 24 % contribution suggested to come from open biomass burning. Ohara et al. (2007), has an distribution in a similar matter with the main source to be domestic(residental) biofuel use and this accounts for 48%. The second largest source is assumed to be industrial burned coal with 19%, followed by transport oil use 14% and domestic coal use 7%. As indicated in Figure 4.4, S2 is the main source in the *ACESS* emission input for CO. The second largest source is S7, road transport, followed by S3, combustion in manufacturing industry, as to the *ACESS* emission follows Streets et al. (2003) rather than Ohara et al. (2007).

Ohara et al. (2007) has no estimates of NMVOC, but the *ACESS* emission distribution for NMVOC follows Streets et al. (2003). As indicated in Figure 4.4 the main source sectors is combustion of coal and biofuels, around 34%, and secondly transportation, with 27%.

The change of sector distributions from the *Original* to the new *ACESS* emission inventory are visualized in Figure 4.4. The main change is that the emission originally distributed in S7, road transport, are in the *ACESS* inventory distributed in S1, combustion in energy and transformation industries, S2, non-industrial combustion plants, and S3, combustion in manufacturing industries. These sectors, and especially S1 and S3 emits the pollution at higher altitudes (see Table 2.1 for the height distribution in different source sectors in the EMEP model). The height distribution can in particularly have an effect on long-range transport and dry deposition.

The replacement of emission input will also give a lower emission output during day. As quantified in Table 2.2, is the day/night distribution in the source sectors. S6, solvent use and other product use, and S7, road transport, emits 3/4 of the emission during day and 1/4 during night. S1, combustion in energy and transformation industry, have an equal day/night emission. S2, non-industrial combustion plants, and S3, combustion in manufacturing industries, have an 1.2 factor during day and 0.8 during night. An effect of the shift in sectors with the *ACESS* emission

inventory can for instance imply a reduction in O_3 production, which is dependent of sunlight.

4.4.2 Spatial distribution of emission

The spatial distributions of the emission totals for the two emission inventories, the *Original* and the *ACESS*, in Asia are visualized in Figure 4.5.

In order to create these figures the emission files were converted from ASCII-files to NetCDF-files, by programming in fortran and using a program called Ferret [1]. The fortran program and ferret-script for converting to NetCDF-files was made available by met.no. Averages of the twelve monthly files were created and Ferret is also used for visualizing the spatial distribution in the average of the emission input data.

As indicated in Figure 4.5, eastern China and parts of Northern India are areas with large sources of emission for all four pollutants. The locations with high emissions is a result of growing industrialization and the growth in population in these areas. The two emission inventories are quite similar and they have both captured the areas with high emissions. It is important to note that the emission value scales in the figures are the same for SO_2, NO_2 and NMVOC, while CO has a higher scale.

Percentage difference

The spatial differences between the two emission inventories are presented in percentage of the *Original* emission ($\frac{ACESS-Original}{Original} * 100\%$). The percentage differences are visualized in Figure 4.6. The scales are identical for the different species and the percentage changes included are 50% in each direction. The reason for the limitation of in the scale is the areas with high percentage difference are most likely areas with no or small amounts of emission in the emission inventories. The difference in percentage can then easily be 100 without providing any meaningful result.
The yellow and red areas are indicate higher emissions in the *ACESS* emission input, light green represent no difference, and the darker green/blue indicate higher emissions in the *Original* inventory. The white areas does not contain data. The squared region in the left corner is part of the EMEP-area, this region has separate emission input files and is therefore not included in the files visualised.

Figure 4.6 shows that areas with the *ACESS* emissions are more centralized in East Asia and in certain areas in for instance India. It is important to note that the *ACESS* emissions are adjusted from the year 2006 to 2000, where the adjustments are taken as a total for the entire area. For instance for Japan, the adjustment factor gives too low emissions, since the emissions here have not increased as much a total of Asian emission. This is part of the reason for lower emissions over Japan in the *ACESS* emissions.

Spatial differences of sector data

The shift from the *Original* emission data to the *ACESS* emission are mainly distributing emission from S7, road transport, to: S1, combustion in energy and transformation industries, S2, non-industrial combustion plants and S3; combustion in manufacturing industries. The sector distribution affects the height the pollutants are emitted in and also day/night distribution.

[1] $http://ferret.pmel.noaa.gov/Ferret/home$

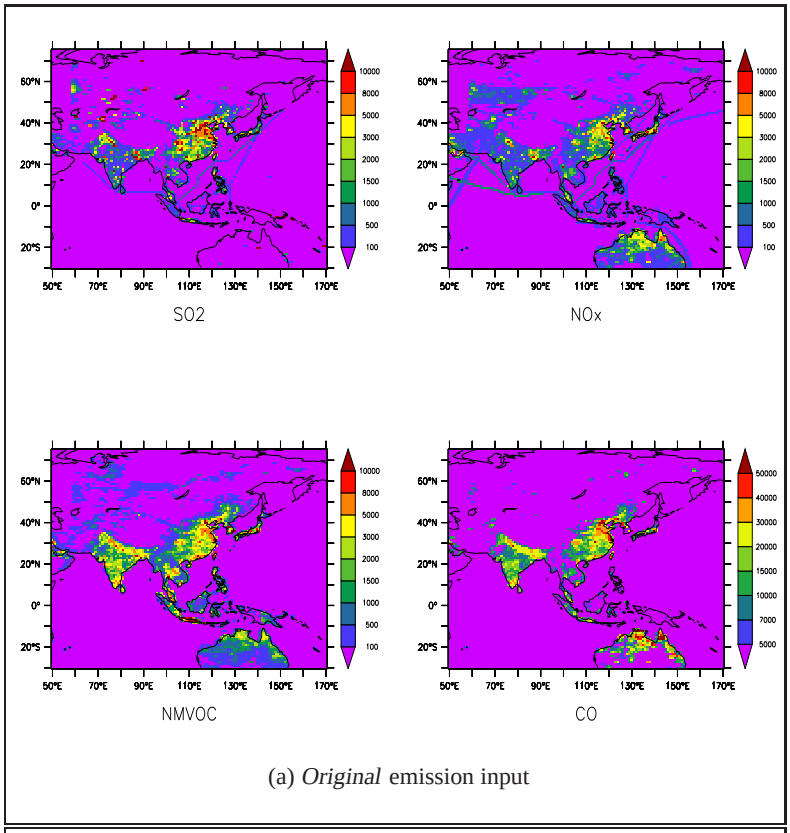

(a) *Original* emission input

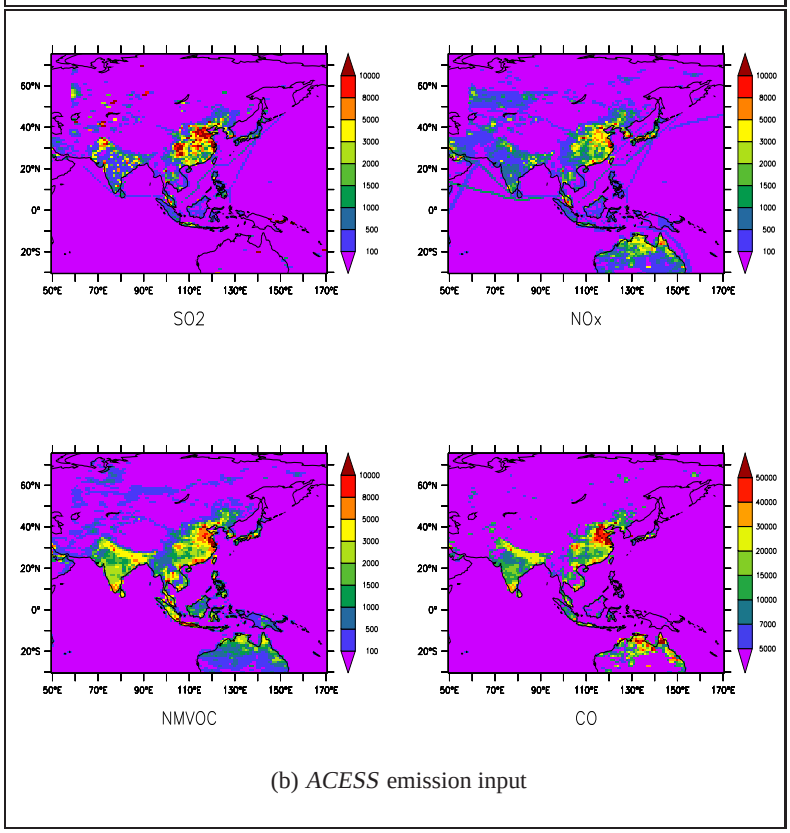

(b) *ACESS* emission input

Figure 4.5: Emission input in the *Original* and the *ACESS* emission inventories of SO_2, NO_x, CO and NMVOC over Asia in 2000 [Gg/month]

In addition, the spatial distribution in these four sectors and these spatial differences are presented individually for the four pollutants, in Figures 4.7 - 4.10. The difference in the following figures and subsections are the *Original* emission data subtracted from the *ACESS* emission, in units of Gg/month. Note that SO_2 and NO_x have the same scale troughout the section, while CO and NMVOC has their own scale. However the scale are kept the same for all sectors.

Figure 4.7 presents the differences in intensities between the yearly totals for the *Original* emission input and the *ACESS* emission input for S1,combustion in energy and transformation industries. The differences are higher in eastern China indicating higher energy use in the *ACESS* emission input., which is according to Ohara et al. (2007) with high emission in Power Plants for China. The height distribution in this sector distributed mostly in between 300 to 1000 meters, this implies that by releasing more emissions at higher altitude the pollution is more sensitive to long-range transport. The day/night distribution shows that the emissions are emitted evenly for day and nighttime, and this affects chemical reactions which are dependent of solar radiation.

Figure 4.8 presents the spatial difference between the *Original* and the *ACESS* emission in S2, non-industrial combustion plants. The figure show greatest differences for CO and NMVOC, especially east China, south in India, Indonesia, and a band north in India and over Nepal. The differences have positive values, which means that the *ACESS* emission input has a higher distribution in this sector. The emissions from S2 are released evenly in the two lowest layers, from surface to 180 meters. The effect of the shift in emissions from S7 to S2 are therefor not that large when considering long-range transport.

For S3, combustion in manufacturing industry, the differences in the spatial distribution be-

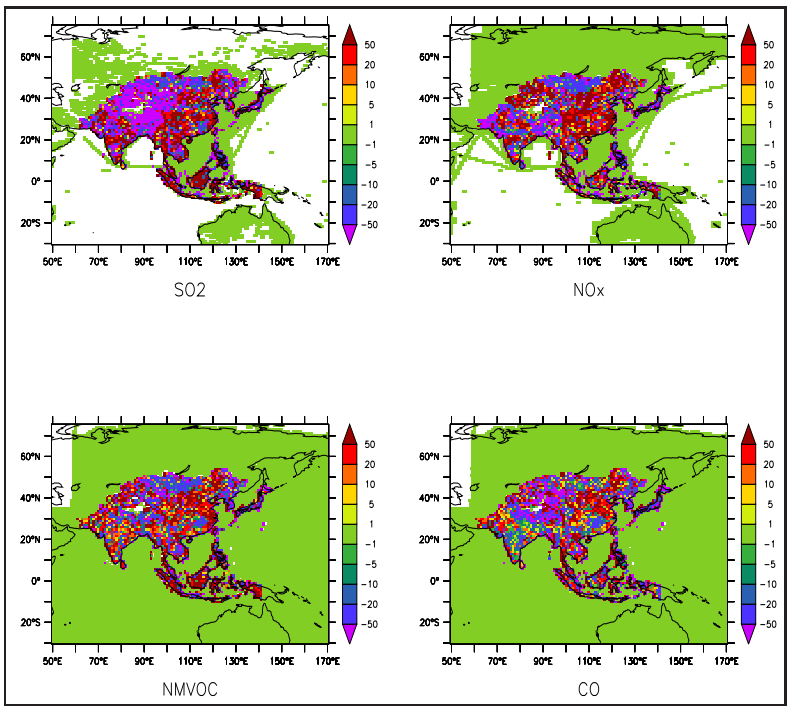

Figure 4.6: Differences in emission input between the *Original* and *ACESS* emission input of SO_2, NO_x, CO and NMVOC in 2000, in percentage of the *Original* emissions.

tween the *Original* and the *ACESS* are presented in Figure 4.9. The figure visualizes higher emissions in the *ACESS* emission data, especially around Beijing; along the coast and further inwards it the country. For the pollutant NMVOC, Japan and some parts of Indonesia are areas of large differences. SO_2 has differences in an area in the west of Pakistan, an area assumed to be the most populated area in Pakistan and where industry is an important source of air pollution.

Figure 4.10 visualizes the spatial differences in the S7, road traffic. The emissions in the figure are mostly negative, which indicates larger emission input in the *Original* data, as expected.
S7, road transport, contains low level emission sources, and the effect of the distribution in higher altitudes in the three sectors described before can be important. The locations are specially sensitive in east China and in the north of India.

Expected effects on model results

As already indicated, there are significant differences in the sector distribution in the two emission inventories the *Original* and the *ACESS* over Asia. This implies differences in the height of the emissions of the pollutants, and also in their diurnal distribution. The *ACESS* emissions over Asia are in general emitted at higher levels, which makes the pollution more sensitive to long-range transport. The temporal effect is a lower emission during day in the *ACESS* emission then the *Original*, which can effect chemical reactions dependent of solar radiation, like O_3 production, and effect the deposition that depends on the stability in the atmosphere. Differences in allocation of the emission are also expected to affect the model results at the individual stations affected by these sources.

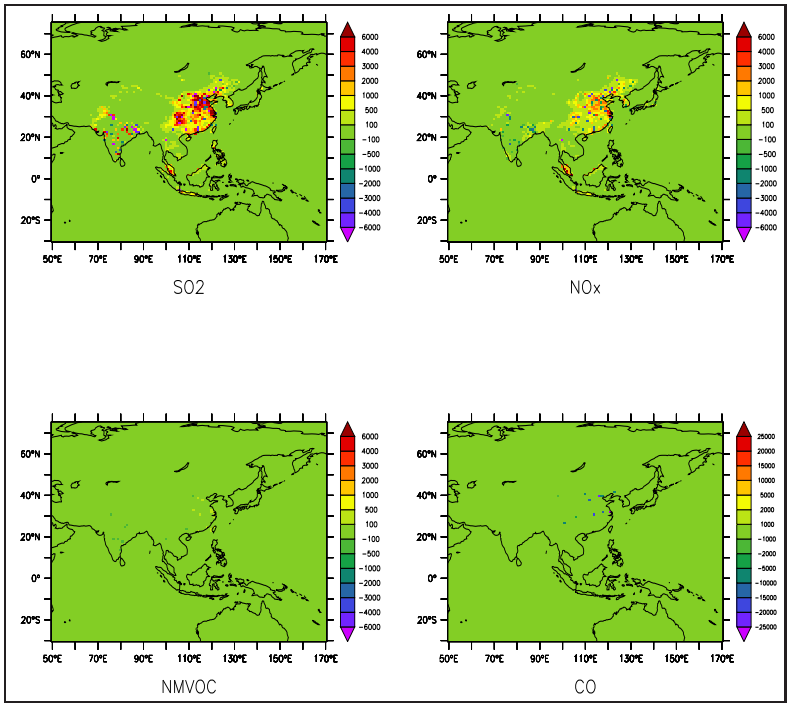

Figure 4.7: Differences in emission input for S1; combustion in energy and transformation industries (*ACESS* - *Original* emission data) [Gg/month]

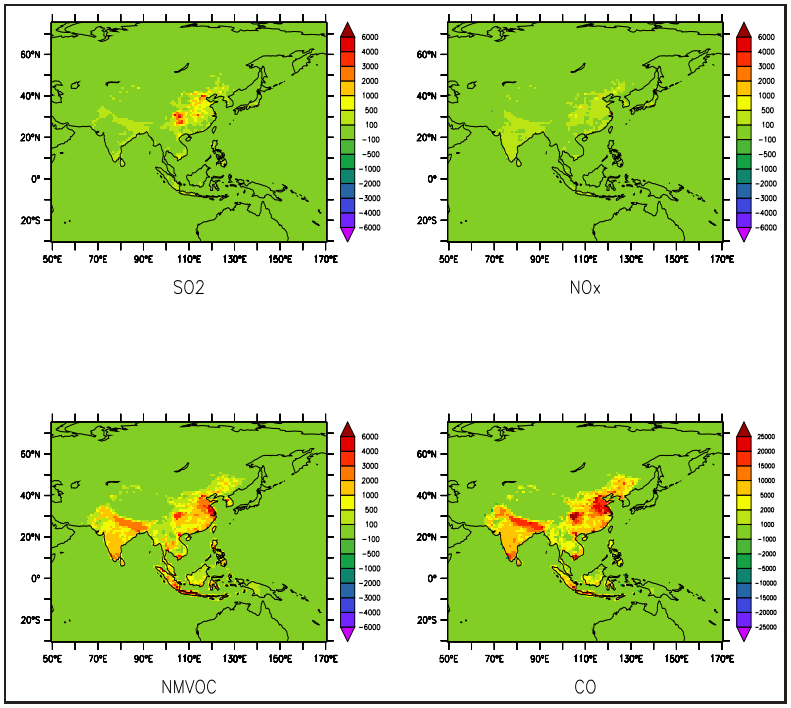

Figure 4.8: Differences in emission input for S2; non-industrial combustion plants (*ACESS - Original* emission data) [Gg/month]

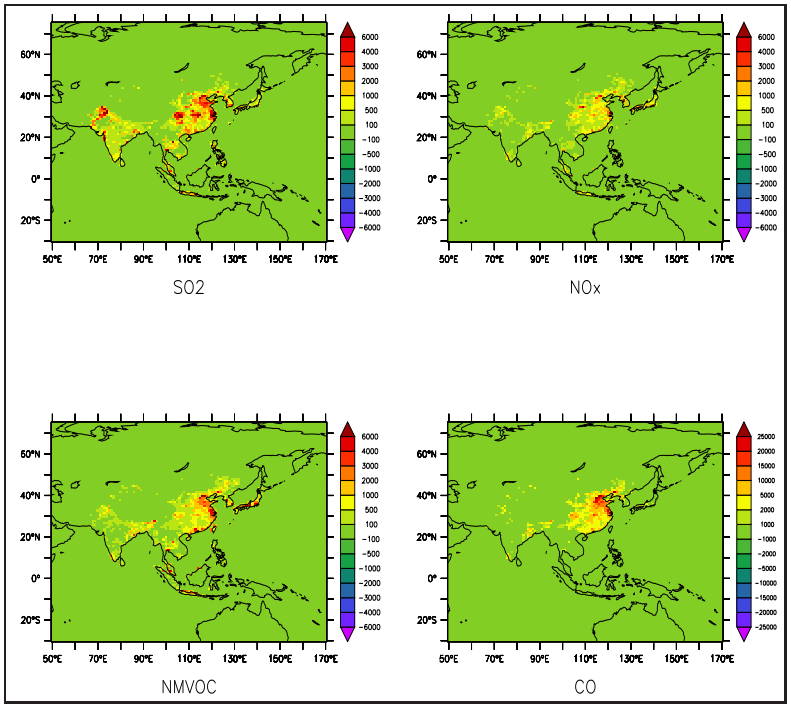

Figure 4.9: Differences in emission input for S3; combustion in manufacturing industry (*ACESS - Original*) [Gg/month]

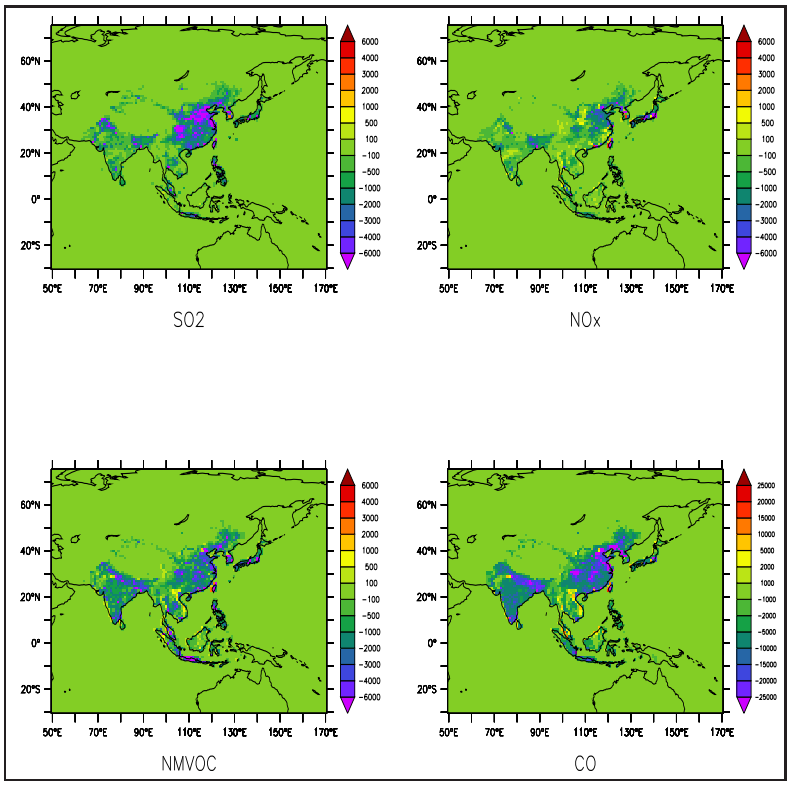

Figure 4.10: Differences in emission input for S7; road transport (*ACESS - Original*) [Gg/month]

Chapter 5

Results

This chapter presents the performance of the global EMEP model for SO_2, NO_2 and O_3 over Asia. These pollutants are of major concern in Asia, with a rapid development in industrialization and an increase in population, and are a danger to regional health and to the ecosystem. The performance of the global EMEP model has been established by comparison with observations from the EANET network over Asia for the year 2001. In addition, the model has been compared with other model results. The global EMEP model has been run with two different emission inventories, to better understand the effects of emissions in model results. The two emission inventories are described in the previous chapter. As shown in the last chapter, the main differences between the two emission inventories are the source sector distribution, which effects the vertical distribution of the emitted pollutants. In general, the new *ACESS* inventory emits pollution at higher levels than the *Original* EMEP global emission inventory.

This chapter presents first the results from the global EMEP model runs. And analyses the differences in SO_2, NO_2 and O_3 air concentrations due to the choice of different emission input. Then, the performance of the global EMEP model against EANET stations are presented, with special attention to distinguish the performance of urban, rural and remote sites. Finally, the results from the global EMEP model are compared with results from eight regional model from the MICS-II study, (Carmichael et al., 2007). The MICS-II study over Asia provides a benchmark for the performance of other chemical transport models in the area. So, the last section in this chapter contains on evaluation of global EMEP model performance compared with the models participation in MICS-II.

5.1 Model results of the global EMEP model in Asia

5.1.1 Spatial distribution

The global EMEP model has been run with two different emission inventories. For convenience the run with the *Original* emission data is called the ***Original run***, and the run with the *ACESS* emission data is called the ***ACESS run*** throughout the thesis.

The spatial distribution of modelled air concentrations are highly affected by input data and especially emission data. The spatial distribution of the two emission inventories in Asia were shown in Figure 4.5. Here, the spatial distribution at surface layer of the two simulations are presented in the figures for the pollutants SO_2 in Figure 5.1, NO_2 in Figure 5.2 and O_3 in Figure 5.3.

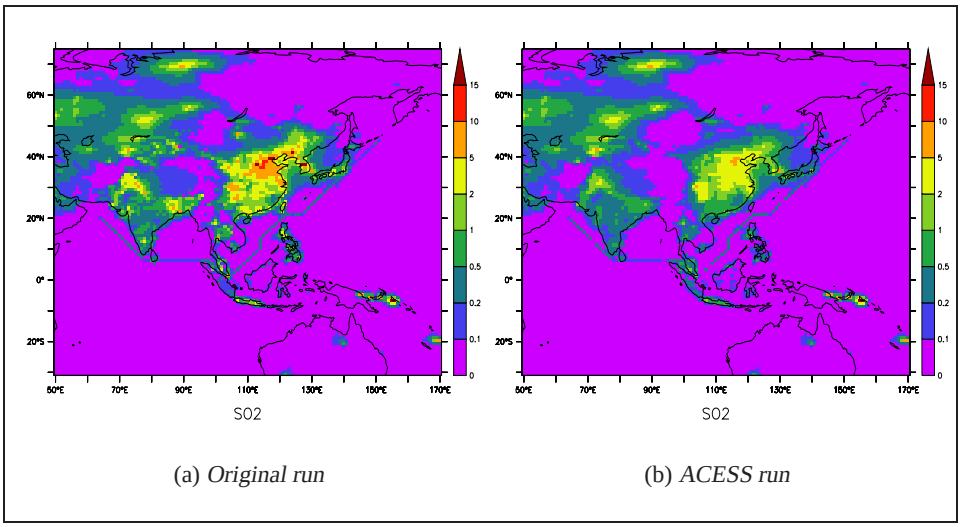

(a) *Original run* (b) *ACESS run*

Figure 5.1: Concentrations of SO_2 at surface layer in the *Original run* and *ACESS run* in Asia 2001 [μSg/m^3].

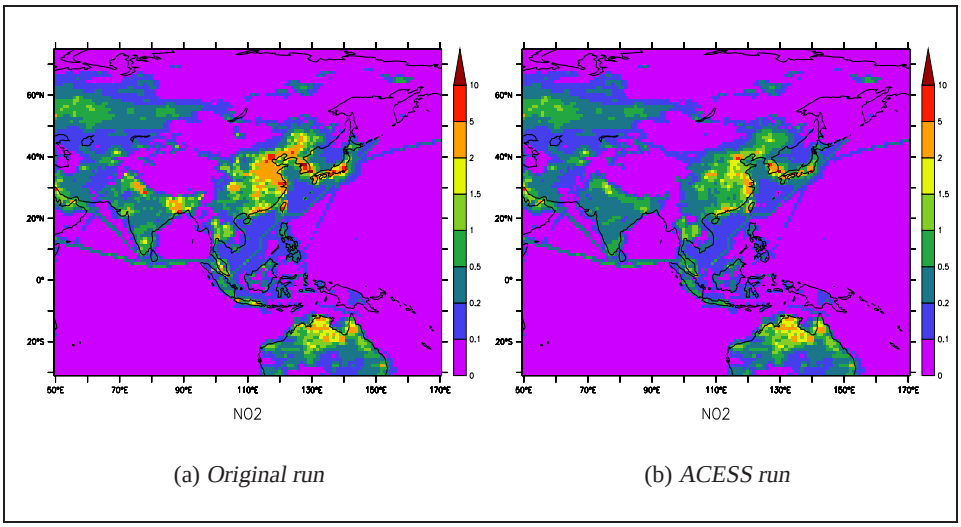

(a) *Original run* (b) *ACESS run*

Figure 5.2: Concentrations of NO_2 at surface layer in the *Original run* and *ACESS run* in Asia 2001 [μNg/m^3].

The spatial distribution of the global EMEP model results for SO_2 and NO_2 air concentrations correspond well with the spatial distribution of SO_2 and NO_2 emissions. The higher levels over China and more moderate levels over Japan reflects the higher emission intensities in the areas in China. SO_2 and NO_2 are primary pollutant, and it is expected that their concentrations show clear resemblance to the emission input data. Note that visualization of the model runs present surface concentration, while the input data is a total of emissions in all heights.

The *Original run* has higher concentrations and covers larger areas than the *ACESS run* at surface layer. This is in spite the impression of higher intensity in the *ACESS* emission input in

some areas. This is related to the vertical distribution of the *ACESS* emission data in higher levels which makes the emission more sensitive to long-range transport. The emissions in the *Original run* are emitted at lower levels, thus the surface simulations of SO_2 and NO_2 in Figure 5.1 and 5.2 are also higher in the *Original run.*

The spatial distribution of O_3 is more complex then for primary pollutants. O_3 is a secondary pollutant and is not emitted directly in the atmosphere in the same way as SO_2 and NO_2, but it is produced by photochemical reactions involving primary pollutants and affected by meteorological conditions, (Commission on Geosciences, 1999). O_3 can be formed by reactions involving volatile organic compounds, VOCs and carbon monoxide in the presence of nitrogen oxides (NO_x=NO+NO_2) and sunlight, for instance see equation 5.1.

$$NO_2 + hv \xrightarrow{O_2} NO + O_3 \tag{5.1}$$

It is important to note that O_3 production can take place in different forms. And also, NO_x is a relevant precursor, however areas with high NO_x intensity can also have a weakening effect of O3 concentrations through NO-titration. NO-titration occurs when emitted NO reacts rapidly with O_3 to produce NO_2 (Sillman, 1999). The equation for this removal is shown in equation 5.2. NO-titration can weaken O_3 production especially during night, wintertime and where there are large power plants - large NO_x emission. NO_x concentrations in power plant plumes are according to Sillmann (2004) often high enough to prevent any O_3 production near the plume source and to cause significant loss of O_3 through NO_x titration. Also in urban areas, under heavy traffic emissions NO_x titration is an effective loss mechanism for O_3.

$$NO + O_3 \rightarrow NO_2 + O_2 \tag{5.2}$$

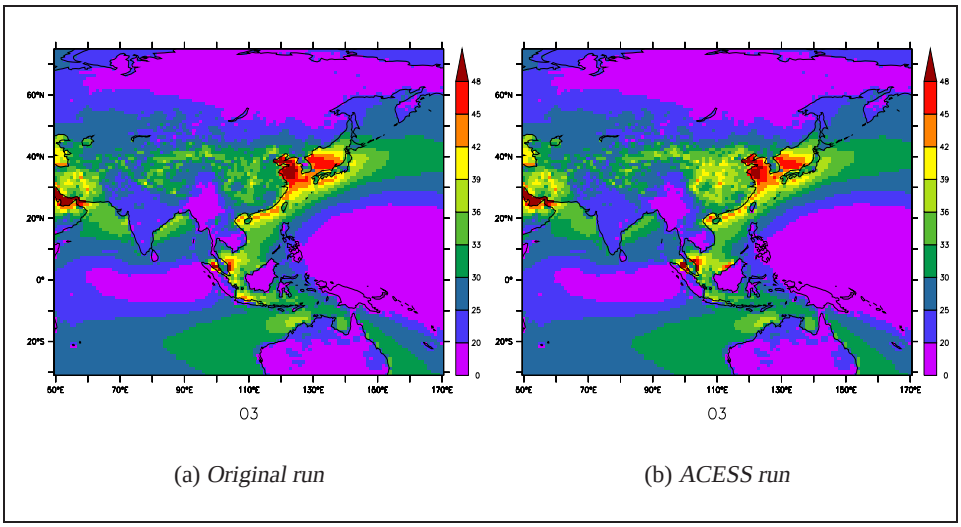

(a) *Original run* (b) *ACESS run*

Figure 5.3: Concentrations of O_3 at surface layer in the *Original run* and *ACESS run* in Asia 2001 [ppb]

Figure 5.3 presents the spatial distribution of O_3 at ground level as calculated by the global EMEP model over Asia, using two different precursor emission data sets. The emission input, in Figure 4.5, is relevant for O_3 formation, especially of NO_x, CO and NMVOC. The model results captures the higher levels of O_3 over Tibet caused by the high level area effected by long-range transport. Areas with high concentrations are found over the Yellow Sea and Sea of Japan, east of the high emission sources in eastern China. The transport pattern east of the high emission sources is due to the continental outflow. The lifetime of O_3 is around 20 days, (Stevenson et al., 2006) and O_3 is sensitive to long-range transport. The high concentrations over the oceans, especially close to high emission sources, are related to the long-range transport of O_3 and the lower deposition of O_3 over ocean. The dry deposition module used in the global EMEP model is described in Simpson et al. (2003), where the base-values of ground-surface resistance for O_3 are different according to land use types. Water has resistance of 2000 s/m, while for instance land use with crops are 200 s/m, urban are 400 s/m and wetlands are 400 s/m. With lower resistance over land the deposition is higher and concentrations shows lower values over land. NO-titration occurring near large emission sources can also be a reason for lower concentrations over land, but this is mostly in relations to high emission sources.

5.1.2 The effect of emission input on surface values

The spatial differences for NO_2 and SO_2 between the *Original run* and the *ACESS run* at ground level are presented in Figure 5.4. The concentrations in the *Original run* are subtracted from the *ACESS run* and the units are in $\mu Sg/m^3$ and $\mu Ng/m^3$, respectively. Differences in the model results are to a large extent affected by the differences in emission input data. For comparison the spatial differences in the emission inputs is included in this section, the *Original* emission subtracted from the *ACESS* emission data, for SO_2 and NO_2, shown in Figure 5.5. Note that the spatial differences in model runs shows the differences in concentrations at the surface level, while the differences in emission input are totals and independent of height.

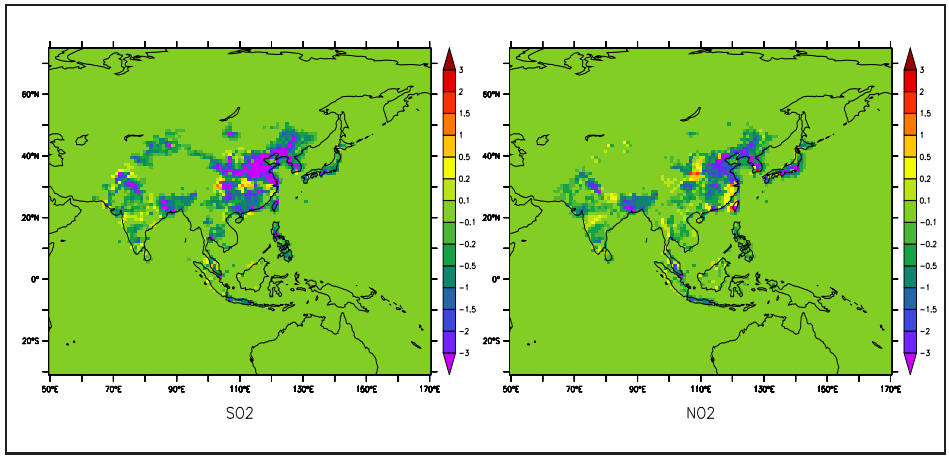

Figure 5.4: Differences in concentrations in surface layer for SO_2 and NO_x : *ACESS run* - *Original run* [$\mu Sg/m^3$][$\mu Ng/m^3$].

In general, for the primary pollutants the differences in the emission input follow the same pattern as the differences in model results. However, the figures indicate higher concentrations in the *Original run* for most areas, like northern parts of India and the majority of East-China.

This is because the vertical distribution of the emissions play a role in the final modelled air concentrations of SO_2 and NO_2. The *Original* input emissions are distributed mostly in S7, road transport, emitted at the lowest layer in the model. In the new *ACESS* inventory the emissions are distributed in four sectors; S1, combustion in energy and transformation industries, S2, non-industrial combustion plants, S3, combustion in manufacturing industries, and S7, road transport. For the vertical differences, especially S1 and S3, release the emissions at higher vertical levels. The spatial differences for the emissions in the four source sectors; S1, S2, S3, and S7, were visualized in chapter 4. By comparing the emission differences in each sector, the emission released at the lowest layer show to be of significant for the modelled surface concentrations for the primary pollutants SO_2 and NO_2.

Figure 5.6 presents the percentage differences at ground level between the *ACESS run* and the *Original run* for NO_2 and SO_2, with the difference taken in percentage of the *Original run.* Note that the scales are ranging from -50 % to 50%, and in this way the high percentage changes are

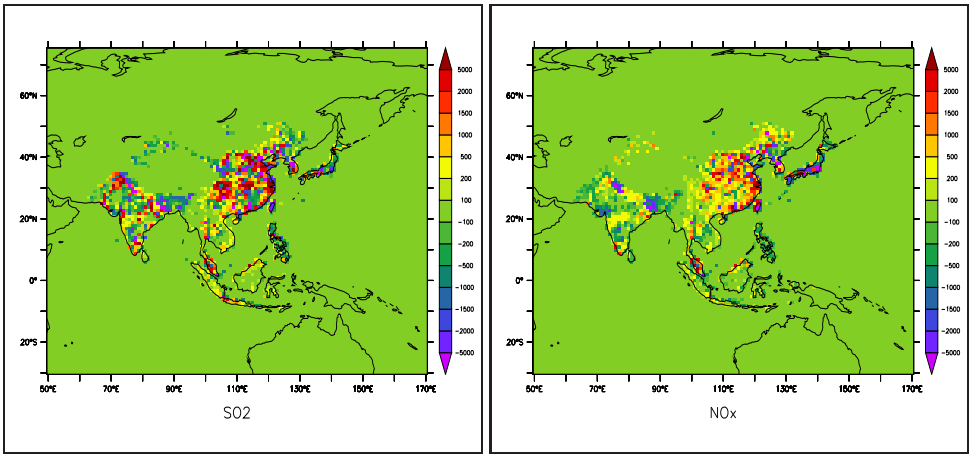

Figure 5.5: Differences in emission input for SO_2 and NO_x : *ACESS - Original* emission input [Tg/month].

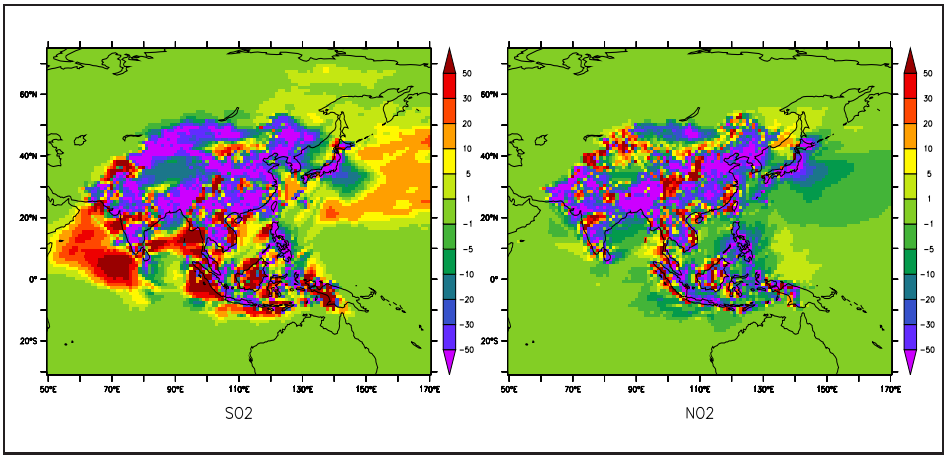

Figure 5.6: The percentage differences in air concentrations at surface level between *ACESS run* and *Original run* for SO_2 and NO_2.

gathered and can be taken under common consideration. These high percentage differences are in general linked to low concentrations and perhaps zero in one model run, which makes the percentage difference up to 100% less meaningful.

As indicated in Figure 5.6, the *ACESS run* has higher percent of SO_2 concentration in ocean areas as a result of more long-range transport. SO_2 has a residence time long enough to be transported over larger areas. The higher percent of the *ACESS run* over oceans is assumed to be reasonable, since more SO_2 is emitted at higher altitudes and is more sensitive to long-range transport. The source sector distribution clearly has an effect on the model runs and over some ocean areas the long-range transport has increased by over 20 %. The land areas are mostly affected by the higher emissions at the lowest layer in the *Original* emission and show a higher percentage concentration in the *Original run.* However, some land regions presents higher percentage concentrations in the *ACESS run.* This is reflecting either more emission in the *ACESS* emission inventory, or areas with low emission sources which are affected by transport in the *ACESS run.* In general, along the coastal areas, larger emissions of SO_2 in the new *ACESS* inventory which is emitted at higher levels, justify the higher SO_2 percentage concentrations over the oceans in the *ACESS run.*

NO_2 shows higher concentrations over ocean areas in the *Original run.* To understand the differences in the performance of NO_2 and SO_2, it is important to remember that the two pollutants have different lifetimes in the atmosphere. The residence time of NO_2 in the lower troposphere is well known to be short (a few hours), while the lifetime of sulphur dioxide molecules in the troposphere is a few days. Since the lifetime for NO_2 is short, it is most likely that the *ACESS* emission, distributed in higher levels, does not have time to be transported with the continental flow over the oceans and down to surface levels. In addition NO_2 is mostly emitted at lower levels, as it originates from traffic, so the differences in the height of emissions due to the correction of sector allocation in the inventory are smaller for NO_2 than SO_2.
In Japan the *Original* emission has higher emissions, which explain the transport of negative percent, the *Original run,* for SO_2 and NO_2 over the sea close to Japan.

In general, the effects of sector distribution in the calculated air concentrations for SO_2 and NO_2 imply differences of 20% or higher over source areas. These are significant differences for SO_2 and NO_2 in air concentrations.

The concentration of O_3 depends on the location and intensity of NO_x, NMVOC and CO precursors emissions and the meteorological conditions. Figure 5.7 presents the spatial differences between the *ACESS run* and the *Original run* in concentrations and percent for O_3. The units are given in ppb, while the percentage visualization is given in percentage of the *Original run.*

Over land areas, for O_3, the air concentrations vary generally below 15 % and show lower differences then for SO_2 and NO_2. Over most of China, Indonesia/Malaysia and regions in India O_3 concentrations are clearly higher in both concentration and percentage difference in the *ACESS run.* While in the ocean areas, parts of India, Bangladesh and Philippines, O_3 concentrations are higher in the *Original run.* The spatial differences in NO_x emission input shown in Figure 5.5, drive the differences in O_3 distribution to a large extent.
The area in eastern China has large emission input in both emission inventories, however, parts of the *ACESS* emission is distributed at higher levels then the *Original* emission data. O_3 con-

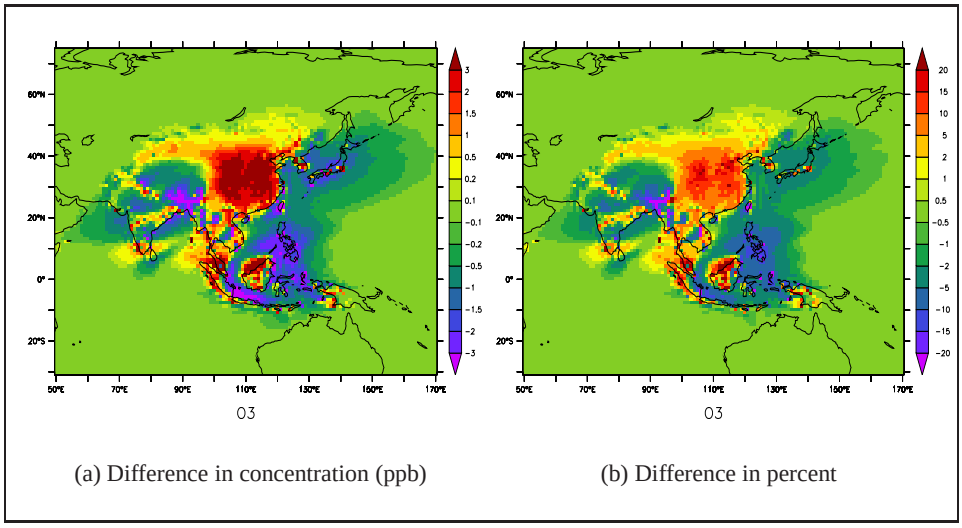

(a) Difference in concentration (ppb) (b) Difference in percent

Figure 5.7: Differences in concentrations and percent in model runs for O_3: *ACESS run - Original run.*

centrations are known to by controlled by the factors of transport, net photochemical production and the removal of O_3, where dry deposition is the major process (Li et al., 2007). Over land areas with high emission sources, especially in east China, have higher O_3 concentrations in the *ACESS run.* This reflects the vertical distribution of emission of NO_x and NMVOC. In the *Original run* the emissions are emitted mostly at lowest layer and are more exposed to dry deposition. By distributing the emission more in the vertical the NO-titration is also weakened, which again confirms the higher concentration in *ACESS run.* The day/night distribution in the source sectors are also a possible reason for higher the *ACESS run* concentrations of O_3. The *ACESS* emits more emission during night, see day/night distribution in table 2.2, when the atmosphere is more stable and there is less dry deposition. However, by emitting more emission during day, as in the *Original* emission inventory, the O_3 production can be higher caused by available solar radiation.

As indicated, the figures from this section shows that the pattern of O_3 concentrations follows to a large extent the NO_2 emission differences.

5.1.3 The effect of emission input at different vertical layers

As mentioned before, the main differences between the two emission inventories are the vertical distribution of the emissions, as a result if the sector allocation. To investigate the effects of the sector distribution, the spatial differences in different heights in the atmosphere are shown in percentage in Figure 5.8. The global EMEP model uses 20 vertical levels, where the first layer, k=1, is the highest layer and k=20 is the layer nearest the ground. In table 2.1 the six lowest layers are presented with the percentage emission emitted in the layers of the different sources sectors. Emission from sector S1, combustion in energy and transformation industries, and S3, combustion in manufacturing industry, are assumed to respectively emit 46% and 41% of the emission in layer k=17, at around 420 meters. And 29 % and 30% in layer k=16, at about 650 meters. The two layers show great similarity in spatial differences of the two model runs, therefore the percentage differences between the model runs are presented only in layer k=16 for SO_2, NO_2 and O_3 in Figure 5.8. This layer is situated within the boundary layer and is expected

to be well mixed. An even higher layer, k=10, at around 2890 meters, is also presented here to illustrate the differences above the boundary layer and in the free troposphere.

The *ACESS run* shows clearly higher concentrations of SO_2 and NO_2 over land areas at layer k=16 (650m), reflecting the vertical emission distribution in the *ACESS* emission inventory. Figure 5.8 shows that SO_2 is transported further with the westerly winds in the *ACESS run* and, at this level the differences in air concentrations of about 20% reaches as far as to North-America. For NO_2 the residence time in the troposphere is lower and the effect of long-range transport has not the same extent as for SO_2. Percentage differences in O_3 concentrations at k=16 (650m) are similar to those in the surface layer, reflecting the mixing in the boundary layer. At level k=10 (2890m), over the boundary layer, the difference in emission inputs are shown to greatly impact the transport of pollution over the Pacific Ocean. In this level the stronger westerly winds carries the pollution emitted at higher levels in the troposphere further. The effect is strongest for SO_2, where the largest shift in sector distribution. A substantial part of the SO_2 emissions were released at higher levels in the *ACESS* inventory, as well as the lifetime for SO_2 is longer than for NO_2. For O_3, changes are driven by NO_2 differences and since it is a secondary pollutant the emission input affects the air concentrations by about 10-15% at k=16 (650m), and at k=10 (2890m) the affects are less significant.

To summarize the spatial difference between the two model results as effects of emission:

- The main difference in the two emission inventories, is that the pollutants in the *ACESS* are emitted at higher vertical levels.
- For primary pollutants, the difference in model result are mostly driven by the differences in emission input, and can account to 20% of surface values.
- The *ACESS run* show an increase in long-range transport, especially for SO_2, and above the boundary layer all pollutants show larger amount of long-range transport.
- The effect of emission sector distribution is largest for SO_2, because SO_2 emissions in the *ACESS* inventory are released mostly at high levels.
- NO_2 is primarily emitted from low traffic sources and has a short residence time in the atmosphere. Therefore, the changes in sector distribution affect NO_2 less than SO_2, except at higher levels in the atmosphere, where the effect of increased emissions from the power sector results in No_2 concentrations.
- O_3 concentrations follows to a large extent NO_2.

5.2 Comparison with observations

The observational data used for comparison and evaluation of the model results are those available from the EANET network in 2001. 15 sites were selected for comparison in this section, where 9 are located in Japan, 4 in China and 2 in Thailand. Note that there are fewer measurements for O_3, with only 10 sites, where 9 are situated in Japan and 1, Samutprakarn, in Thailand (see Figure 3.1 for location of the sites in Asia). The evaluation of the global EMEP model has been made on the basis of the analysis of yearly mean concentrations, correlation, bias and time series evaluated in urban, rural and remote sites. The location of the measurements can affect

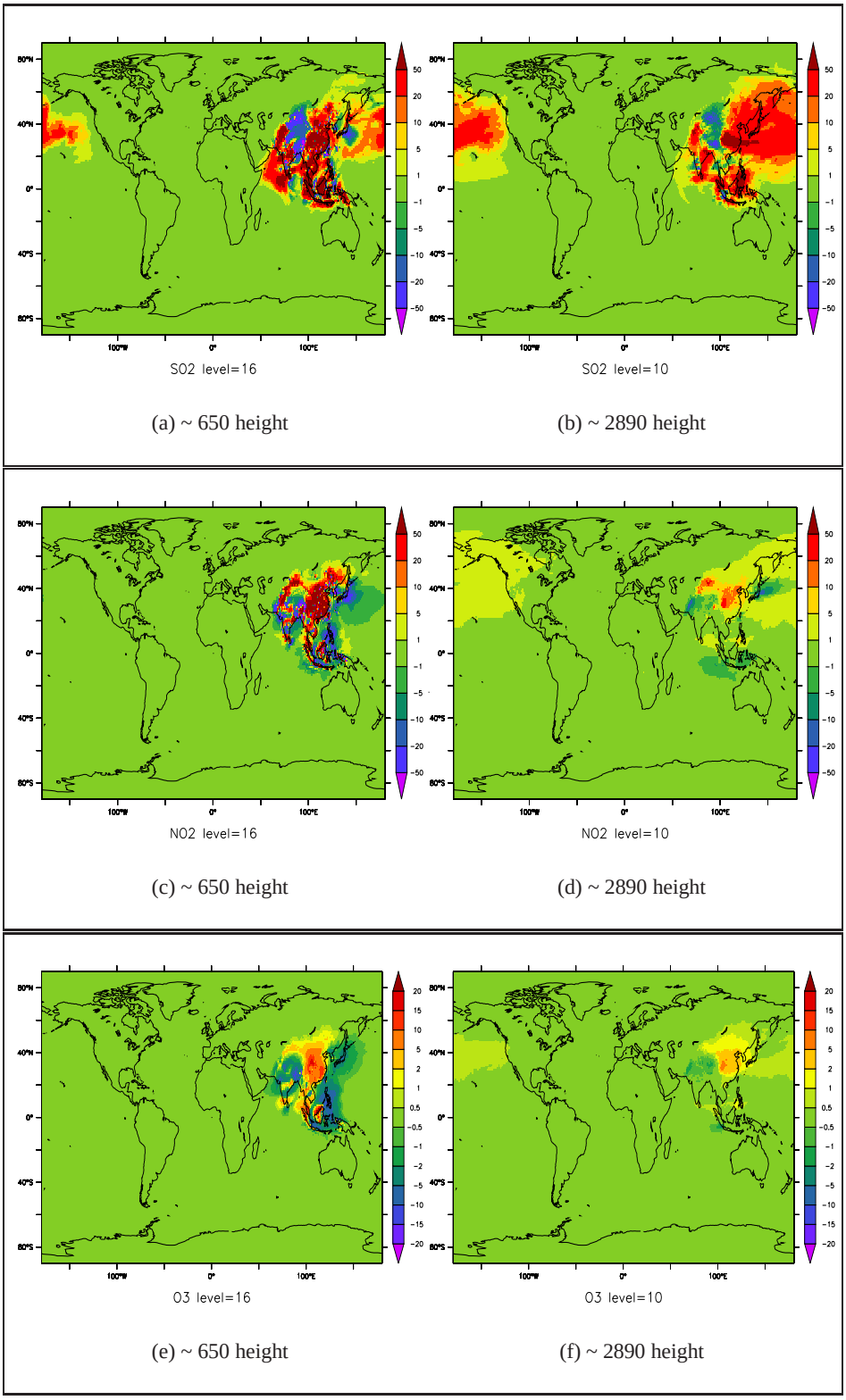

(a) ~ 650 height (b) ~ 2890 height

(c) ~ 650 height (d) ~ 2890 height

(e) ~ 650 height (f) ~ 2890 height

Figure 5.8: Percentage differences in concentrations between model results, *ACESS run - Original run*, taken in percentage of *Original run* in different vertical layers. The top panel shows SO_2 concentration, and the middle and lower panel show NO_2 and O_3, respectively. The left side is at level k=16(~ 650 height), while the right side is at level k=10(~ 2890 height)

the correlation with the model results and before comparing the model results with observations, urban, rural and remote sites are described, and the expected model performance, especially for primary pollutants, is discussed.

The global EMEP model has a grid resolution pf 1°x1°, which is approximately a horizontal resolution of 110 x 110 km^2. The area can include emission sources of different intensities. The model assumes an average value for the whole grid area, and the placement of the measurement site inside the grid area has an effect on the comparison with model results. For instance, the comparison with the modelled grid averaged and the measurement site, will not be the same whether the site is near a large power plant or if it is a remote site far from sources.

The EANET network distinguishes 3 types of sites; urban, rural and remote.
An urban site is located in an industrial area and situated close to emission source, most likely cities. The model average of the entire grid area can include both high emission sources and more remote areas. The model simulations are most likely not able to capture the concentration peak measured in urban sites. The model is therefore expected to underestimate the pollutants concentration observed in urban sites.

Secondly, a rural site is, according to EANET, a site that must be more than 20 kilometers away from large pollution sources. The concentration in a rural site depends on meteorology and the components chemical characteristics in the atmosphere. The direction of the wind, the lifetime of the component, and chemical reactions affects the air concentration in the grid area. The model averages over an area of about 110 x 110 km^2, which is large compared the distance of 20 kilometer between the measurement and high pollution sources. It is therefore expected that it will be possible errors in the model simulations when comparing with observations in these sited, caused by the coarse grid mesh.

Remote sites in EANET must be located more than 50 kilometers away from large pollution sources, and also more than 500 meters from main roads. The remote sites are, according to EANET's classification and in spatial sense, the site least affected by emission sources. At what extent the emission sources in the vicinity impact the site depend, like for rural sites, on meteorology and chemical processes in the atmosphere. These sites are the most adequate sites to compare with in a model with grid resolutions of 50-100 km.

In this thesis, the performance of the global EMEP model has been compared with observations from all these types of sites, recognizing the limitations of a comparison of a coarse resolution model with urban/local stations.

5.2.1 Yearly mean for urban, rural and remote stations

SO_2

Table 5.1 gives the comparison of SO_2 yearly mean values of surface concentration and the correlation of modelled versus observed air concentrations for the different sites in Asia 2001. The observations shows a general gradient in concentrations for the urban/rural sites with higher mean values than remote sites. The exceptions are the urban cite Banryu and rural site Ijira, both situated in Japan. This reflects the emission intensities in Japan compared to China and Thailand, since air concentrations in Japan are generally lower than in China. China clearly has the highest emission sources of SO_2, and the three sites; Jinyunshan, Hongwen and Xiang-Zhou,

	Site	Observation	*Original run*	Corr.	*ACESS run*	Corr.
Urban	6: Hongwen (China)	11.38	0.96	0.20	0.84	0.27
	8: Xiang-Zhou (China)	13.30	2.06	0.30	1.27	0.30
	23: Banryu (Japan)	1.33	0.55	0.05	0.49	0.07
	37: Bangkok (Thailand)	3.84	0.84	0.06	0.65	0.18
	38: Samutprakarn (Thailand)	6.24	0.88	-0.22	0.66	-0.28
Rural	2: Jinyunshan (China)	13.24	6.73	0.20	4.91	0.25
	4: Weishuiyuan (China)	6.80	9.90	0.02	3.36	0.08
	22: Ijira (Japan)	1.22	0.62	0.16	0.23	0.08
Remote	14: Rishiri (Japan)	0.26	0.06	0.23	0.07	0.25
	15: Tappi (Japan)	0.58	0.11	0.26	0.09	0.26
	17: Sado (Japan)	0.83	0.13	0.32	0.10	0.20
	18: Happo (Japan)	0.97	0.58	0.04	0.25	0.02
	19: Oki (Japan)	0.84	0.30	0.17	0.26	0.18
	20: Yusuhara (Japan)	1.50	0.95	0.02	0.74	0.06
	21: Hedo (Japan)	0.40	0.29	0.04	0.11	0.17

Table 5.1: Observations of SO_2 concentrations at different sites in Asia compared with model results [μgS/m^3].

have SO_2 concentrations over 10 μgS/m^3 as annual mean.

Table 5.1 presents mean modelled values and temporal correlations with observations for the *Original run* and the *ACESS run.* In general SO_2 concentrations are underestimated in both model runs, as is expected since the stations, especially urban and rural, are close to emission sources and the model grid is coarse. The exception is Weishuiyuan with an overestimation in the *Original run*, which reflects the higher *Original* emission input in this region. The *Original run* has in general higher SO_2 mean concentrations in the selected sites. Figure 4.6 gives the percentage spatial difference between the *Original* input and the *ACESS* input data. The areas with higher *Original* emission input of SO_2 reflects higher concentrations in the *Original run*, and the same for the *ACESS* emission data and the *ACESS run.* Figure 4.6 implies higher input of *Original* emissions over large parts of Japan, which is assumed to be the reason for the higher concentration in the *Original run* for most of the sites located here.

In general, the global EMEP model performs better for the rural and remote sites compared with observations. Table 5.4 presents an overview of the bias calculated for all pollutants analysed and the two model runs in the different sites. The mean bias is calculated for the different site categories and totals ($\frac{mean\ model\ result - mean\ observation}{mean\ observation} * 100\%$).
Table 5.4 shows generally a negative bias for SO_2 concentrations. This is expected because of the coarse resolution and the poor representativeness of observations. SO_2 has a mean bias of -50% in the *Original run*, and -66% in the *ACESS run.* The regional EMEP model simulations over Europe had mean bias that varied from 18% to 60% over the last ten years (Simpson et al., 2006; Fagerli and Aas, 2008; Jonson et al., 2006). This shows the results over Asia to be highly underestimated, while it is overestimated in Europe. The overestimation over Europe is related to the high representativeness of remote sites, and SO_2 emissions mainly emitted by point sources, reflecting the overestimation in mean bias over Europe.
The remote sites are expected to be most adequate for comparison between model results and

observations in such coarse resolution model as the global EMEP model. However, the global EMEP model show substantial underestimation also in remote sites. This can be a result of the fact that all the remote sites are situated in Japan, which makes the spatial basis of comparison scarce and biases the results. This can be related to low emission input over Japan. For the *ACESS* emission data, the adjustment from 2006 to 2000 (described in chapter 4) probably resulted in too low emissions in the *ACESS* emission over Japan. This can cause underestimation of SO_2 concentrations in the remote sites in Japan in the *ACESS run.*

The site with the better agreement between the model results and the measured SO_2 mean concentration is Hedo, in Japan. This remote site is located on an island in the East China Sea. The grid box in the model includes no other high sources then the ones located on the island, which can be the reason why the model results are in good agreement with the measurements.

The temporal correlations of modelled and observed values are generally low, which is expected since there is no seasonal variation included in the emission data, and considering the models coarse grid resolution.
However, the *ACESS run* has a higher correlation in most sites. The differences are small, but it indicates that the global EMEP model performs better with the new *ACESS* emission data. The sector distribution, with pollutants emitted at higher levels, has an effect on the model results. Here the remote sites shows the best correlation, which is expected considering the models resolution. The mean temporal correlation for the *Original run* was calculated to 0.123 and for the *ACESS run* the mean correlation was 0.139, and for only the remote sites the mean correlation was 0.154 and 0.163, for the *Original run* and the *ACESS run*, respectively.
Mean spatial correlations for the regional EMEP model over Europe show higher values of correlation, vary from 0.43 to 0.78 the last ten year (Simpson et al., 2006; Fagerli and Aas, 2008). The lower correlations over Asia, is caused by several reasons. Like that the values over Europe are spatial correlations, compared to the temporal correlations calculated over Asia, and the spatial correlations are expected to be higher. As well as the coarse resolution in the global EMEP model, compared to the finer grid in the regional EMEP model (50 x 50 km^2). No seasonal variation is included in Asian emission input, and the low representativeness of observations in Asia, are also reasons that must be considered when comparing the correlation over Europe and Asia.

NO_2

Table 5.2 presents the values for the observation and the modelled results of mean NO_2 concentrations, as well as temporal correlations in the selected sites over Asia for 2001. Urban and rural sites show high concentrations of NO_2, especially Bangkok, Samutprakarn and Xiang-Zhou. These sites are situated close to cities like Bangkok or Hong-Kong, near high emissions sources. The model runs have not manage to reproduced the high concentrations in the sites, which is reasonable considering the models coarse grid resolution.

The model results generally underestimate the observed NO_2 concentrations. However, at the rural sites Jinyunshan, in China, and Ijira, in Japan, and remote sites Happo, Yusuhara and Hedo, in Japan, NO_2 concentrations are overestimated in the *Original run.* The *ACESS run* overestimate the NO_2 concentration in urban site Weishuiyuan in China, reflecting the spatial differences in the emission input data.

Table 5.4 shows negative bias for NO_2 concentration in most sites. This is expected because

	Site	Observation	*Original run*	Corr.	*ACESS run*	Corr.
Urban	6: Hongwen (China)	6.61	0.99	0.10	1.22	0.15
	8: Xiang-Zhou (China)	10.87	2.47	0.19	2.83	0.20
	23: Banryu (Japan)	2.33	0.82	0.06	0.88	0.07
	37: Bangkok (Thailand)	14.70	1.10	0.25	1.30	0.29
	38: Samutprakarn (Thailand)	11.49	1.12	0.39	1.31	0.43
Rural	2: Jinyunshan (China)	1.60	2.00	0.15	1.11	0.14
	4: Weishuiyuan (China)	2.69	2.51	-0.07	4.16	-0.07
	23: Ijira (Japan)	1.81	2.48	0.42	1.15	0.40
Remote	14: Rishiri (Japan)	0.40	0.09	-0.06	0.09	0.00
	15: Tappi (Japan)	0.67	0.18	0.18	0.15	0.20
	17: Sado (Japan)	0.63	0.21	0.23	0.17	0.22
	18: Happo (Japan)	0.86	1.77	0.34	0.96	0.31
	19: Oki (Japan)	0.77	0.45	0.10	0.41	0.08
	20: Yusuhara (Japan)	0.93	1.70	0.12	1.53	0.27
	21: Hedo (Japan)	0.44	0.52	0.04	0.35	0.08

Table 5.2: Observations of NO_2 concentrations at different sites in Asia compared with model results [μgN/m^3].

of the coarse resolution and the poor representativeness of observations. However, there is a difference between urban, rural and remote sites.

NO_2 has a mean bias of -86%, 15% and 5% for urban, rural and remote sites, in the *Original run*, with a mean bias for all sites of -68%. The *ACESS run* had mean bias calculated to -84%, 5% and -9% for urban, rural and remote, respectively, and with a total mean bias of -69%. The mean bias over Europe for the last ten years, varied from -8% to 18%, (Simpson et al., 2006; Fagerli and Aas, 2008; Jonson et al., 2006). The global EMEP model show poorer performance over Asia than the regional model over Europe. However, there is a clear difference in the bias according to the site classification, where the global EMEP model show better skills in rural and remote sites, as expected.

The *ACESS run* calculates better the NO_2 concentrations at urban sites and at the rural site Ijira in Japan. While the *Original run* has better results for remote sites and the remaining rural sites. The reason why the *ACESS run* shows lower NO_2 concentrations in remote sites, are related to the lower emission input over Japan in the *ACESS* emission input.

The *ACESS run* shows generally higher values of temporal correlations for NO_2 than the *Original run.* The more detailed source sector distribution in the *ACESS* emission contributes to a better performance of the global EMEP model. The mean correlation in the *ACESS run* is 0.185 and for the *Original run*: 0.163. Comparing with calculations from the regional EMEP model over Europe, is the modelled correlation over Asia significantly lower. From the last ten years the mean spatial correlation in the Europe varies from 0.45 to 0.80 (Simpson et al., 2006; Fagerli and Aas, 2008; Jonson et al., 2006). It must be noted that these values are spatial correlations and are usually higher than temporal correlations. The stations in Europe are all remote sites and well distributed, in contrast to the scarce observation data available over Asia. This, as well as no seasonal variation in emission data and coarser grid resolution, are why it is, as expected, a better performance of the EMEP model in Europe than in Asia.

O_3

Table 5.3 presents a comparison of the mean yearly values for O_3 in ppb for the observation and model runs, and the temporal correlation for the selected sites in Asia 2001. Note that there are fewer measurement sites for O_3, with observation data presented from 10 sites, where 9 are located in Japan, only Samutprakarn is located in Thailand.

	Site	Observation	*Original run*	Corr.	*ACESS run*	Corr.
Urban	23: Banryu (Japan)	36.11	42.70	0.30	41.99	0.30
	38: Samutprakarn (Thailand)	4.52	21.80	0.10	22.92	0.13
Rural	22: Ijira (Japan)	29.65	32.51	0.13	31.71	0.17
Remote	14: Rishiri (Japan)	38.13	33.10	0.56	32.49	0.58
	15: Tappi (Japan)	46.56	37.61	0.64	36.80	0.67
	17: Sado (Japan)	41.02	43.64	0.52	42.73	0.56
	18: Happo (Japan)	53.29	35.96	0.25	34.8	0.31
	19: Oki (Japan)	44.62	45.14	0.52	44.64	0.49
	20: Yusuhara (Japan)	28.91	33.76	0.29	32.63	0.30
	21: Hedo (Japan)	42.89	34.53	0.67	33.92	0.68

Table 5.3: Observations of O_3 concentrations at different sites in Asia compared with model results [ppb].

The measured O_3 concentrations does not differ for urban, rural and remote in the same way as for the primary pollutant SO_2 and NO_2. The model results are in somewhat better agreement with observations. The highest concentrations are measured in the remote sites. These sites are affected by long-range transport of O_3 concentrations, as well as the effect of NO-titration being not that significant for areas outside of large emission sources.
The urban site Samutprakarn has a mean yearly observation at 4.52 ppb, which is very low. It is not clear if there are some errors in the measurements at Samutprakarn.

O_3 concentrations have less observational data than for SO_2 and NO_2. The mean bias calculated for the sites in Table 5.4, except for Samutprakarn, since the credibility of the site observation is questionable, gave mean bias in the *Original run* of -6%. And in the *ACESS run* a mean bias of -8%. Compared to simulations of SO_2 and NO_2 concentrations, the global EMEP model show best skills in calculating the O_3 concentration for both model runs.

Table 5.3 shows the temporal correlation to be improved for all sites in the *ACESS run.* The mean correlation in the *ACESS run* was calculated to be 0.419, and for the *Original run* the mean correlation was found to be 0.398. Table 5.3 also indicates higher correlation in remote sites, with a mean correlation in these sites of 0.493 and 0.513 for the *Original run* and the *ACESS run,* respectively. The higher correlation for O_3 concentrations are related to the fact that O_3 is a secondary pollutant. It is not primarily effected by the emission input and it is sensitive to long-range transport. The mean correlation in the *ACESS run* is slightly better, indicating that the emissions are better distributed in the *ACESS* emission input. The more detailed the source sectors distribution show to improve the model performance. The higher correlations in remote sites are in agreement with what is expected. However, comparing to European values, where the correlation often exceeding 0.8 (Fagerli et al., 2003), the values found for Asia are clearly lower. Still, factors like poor representativeness in observations over Asia and coarser

Site	SO_2		NO_2		O_3	
	Original run	*ACESS run*	*Original run*	*ACESS run*	*Original run*	*ACESS run*
Hongwen	-92%	-93%	-85%	-82%		
Xiang-Zhou	-85%	-90%	-77%	-74%		
Banryu	-59%	-63%	-65%	-62%	18%	16%
Bangkok	-78%	-83%	-93%	-91%		
Samutprakarn	-86%	-89%	-90%	-89%	382%	407%
Jinyunshan	-49%	-63%	25%	-32%		
Weishuiyuan	46%	-51%	-7%	55%		
Ijira	-49%	-81%	37%	-36%	10%	7%
Rishiri	-77%	-73%	-78%	-78%	-13%	-15%
Tappi	-81%	-84%	-73%	-78%	-19%	-21 %
Sado	-84%	-88%	-67%	-73%	6%	2%
Happo	-40%	-74%	106%	12%	-33%	-35%
Oki	-64%	-69%	-42%	-47%	1%	0%
Yusuhara	-37%	-51%	83%	65%	8%	6%
Hedo	-28%	-73%	18%	-20%	-19%	-21%

Table 5.4: Bias in the *Original run* and *ACESS run* in different sites in Asia 2001.

grid resolution, are some of the reasons for the substantial difference in correlation.

5.2.2 Time series variations for urban, rural and remote sites

Time series of daily concentrations of SO_2, NO_2 and O_3 in certain urban, rural and remote sites are presented in this section for the year 2001. This shows the temporal performance of the model.
In all the figures presented in this section, the black line represents the observations, the blue line corresponds to the model result from the *Original run* [Original], and the red line shows the results from the *ACESS run* [ACESS]. Figures with periods without black line, indicates lack of representative observation data.

The meteorology pattern in Asia is highly relevant for the seasonal variations in the measurements and simulations the sites. During wintertime the atmospheric transport with emissions from China over Japan is more important. In the winter a high pressure center is situated over the inland of Asia, called the Siberian high. This high pressure system is creating an anticyclonic circulations, which transports air out over the ocean areas. In the summer, a low pressure is situated over Central Asia, then the East Asian monsoon brings clean air from the Pacific Ocean, (Pochanart et al., 2004). Another relevant factor is the cold climate during the wintertime in mainland China, which gives rise to the need for heating and energy production. This is important for understanding the higher emission of SO_2 during the cold periods.

Urban sites

This section analyses the time series variations at the urban sites; Banryu, in Japan, and Samutprakarn, near Bangkok in Thailand, as shown in Figure 5.9. Banryu [Banr], (34 °04' N, 131 °42'), is located on the west coast in the south of Japan. The site is at a lake and 60 meters above sea level. Samutprakarn [Samu], (13 °44' N, 100 °34' E), is by a small province only 2 meters over

sea level, between Bangkok and the sea to the south.

The variations of SO_2 and NO_2 air measurements at Banryu presents higher concentrations in winter than in summer. The meteorological pattern and seasonal variations described earlier, are valid for interpreting the observations from this site that shows the effect of long-range transport from China during winter. Although the model results capture the main variation with higher concentrations during winter, the temporal correlation is low because of the poor daily covariance.
The seasonal variations in the model results of O_3 concentrations at Banryu are in good agreement with the observed variations.
The same seasonal variation as in Banryu is not seen for SO_2 concentrations in Samutprakarn, where high concentrations are observed during summer instead of winter. It is possible that the location of the site makes it vulnerable to pollution from Malaysia and Indonesia when the summer monsoon transports air from the south. The correlations for both model runs in Samutprakarn is negative and is related to the models calculations of lower concentrations during summer. The model does not capture the plumes in the observations in June, July and August. The lack of a convection scheme in the EMEP model can be an important factor here. However, for NO_2 the seasonal correlations in the model runs are high, considering no seasonal variation in emission input, with a value of 0.43 in the *ACESS run.*

The O_3 concentration at Samutprakarn is very low with a mean of 4.52 ppb, and the model results highly overestimates the concentrations. The temporal variations in Figure 5.9 shows the low measurements to be under 10 ppb for the whole year. Samutprakarn has a very high NO_2 concentration and the effect of NO-titration, where emitted NO reacts rapidly with O_3 to produce NO_2, can weaken the O_3 values drastically. However, the O_3 concentrations are very low and it is possible the observations contains errors.
The model simulations at Samutprakarn shows a seasonal variation with lower O_3 concentrations during summer. It it possible that the summer monsoon creates a lot of cloudiness. The solar radiation in the EMEP model is calculated at every time-step for the deposition calculations, and for photolysis rates. These calculations are based upon variables like the models cloud cover, (Simpson et al., 2003). By decreasing the solar radiation when clouds are present, the O_3 production is also reduced, which can account for the lower O_3 concentrations during the summer.

Rural sites

The observations from EANET included three rural sites, Jinyunshan (Chongqing) and Weishuiyuan (Xiàn) in China, and Ijira in Japan. The 2001 times series for Weishuiyuan and Ijira are plotted in Figure 5.10.
Weishuiyuan [Weis], (34 °22'N, 108 °57'E), is located 360 metes above sea level in the Xiàn area and is the capital of the Shaanxi province in the China. Ijira [Ijir], (35 °34'N, of 136 °42'E), is situated at a lake in the island Honshu in Japan, 140 meters high.

The *ACESS run* overestimates NO_2 concentrations in Weishuiyuan, and underestimates the concentrations of SO_2. While the *Original run* presents the opposite scenario, with underestimation of NO_2 and overestimation of SO_2 concentrations. Differences in emission input (Figure 5.5) reflect the model results and show higher SO_2 emission over Weishuiyuan in the *Original* input. And higher NO_2 emission over Weishuiyuan in the *ACESS* input. The emission input data is clearly affecting the model results. This is as expected from a coarse model in a rural site.

Weishuiyuan has a high peak in the observations in March for both NO_2 and SO_2 concentrations. The peak reaches to 50 $\mu Sg/m^3$ and 20 $\mu Ng/m^3$, and is most likely caused by a plume in the area at that time. The site Jinyunshan, further south of Weishuiyuan has observed the same peak. Here the concentrations are as high as over 80 $\mu Sg/m^3$ for SO_2 and 20 $\mu Ng/m^3$ for NO_2. The meteorology is an important factor, and from other experiments it seems that different sites in China had several peaks during this month, (Wang et al., 2005). Early spring is a transition period in between the summer and winter monsoons and therefore there can be a period where the Siberian high and the Pacific low comes and goes (Bey et al., 2001). As mentioned before, during winter the meteorology is dominated by the high pressure over Siberia and the Aleutian low over the Pacific ocean. Over eastern China early spring is characterized by frequent passages of strong cold fronts. These fronts are moving towards south over northern China and Korea. When it comes to March the high-pressure in the Pacific is building up and the Siberian high get weaker. Now a warmer and more tropical air from the south is more frequent. At this time the convergence becomes more apparent, and this has an important impact on the export of pollution from the Asian continent (Bey et al., 2001).
The temporal correlations at Weishuiyuan in Figure 5.10 are low for both model results, and for NO_2 the correlations are even negative. Seasonal variations of observations in the Weishuiyuan show higher values during summer, especially in June. The model results shows a variation described earlier with lower emission during summer causing a negative correlation.

Ijira shows model results in better agreement with the observation of NO_2 concentrations, and also the correlation is better when compared to the other sites. There is however an overestimation of the NO_2 concentrations in the *Original run*, this reflects the emission input.
Observations of SO_2 at Ijira show frequent peaks in the concentrations from April to August. The summer monsoon creates a transport of marine air from the Pacific. The peaks in the SO_2 concentrations at Ijira can have related to these winds from the south, where the Chukyo Industrial area is located near the city Nagoya, Sase, Ohizumi, Nakayama, Peng, and Ueda (Sase et al.). To a high extent these plumes are not captured by the model simulations, and the correlation for both model runs are low. This is most likely related to transport processes not reproduced by the model. The global EMEP model does not include a convection scheme. This limitation can effect both horizontal and vertical transport, and can be a reason for the models low correlation. The global EMEP model show good performance in simulating the O_3 concentrations at Ijira.

Remote sites

In this subsection the time series for model and observations in the remote sites Hedo and mountain site Happo, both situated in Japan, are shown in Figure 5.11. Hedo [Hedo], (26 °09'N, 128 °03'E), is located on an island south of the mainland of Japan in the East China Sea, 60 meters above sea level. Happo [Happ], (36 °41'N, 137 °48'E), is a high level site, 1850 meters above sea level, situated on the west coast of Japan. Note that when converting the units in the observations for most sites an assumption of a temperature of 20 ° C and pressure of 1013 hPa was made. While Happo was assumed to have a temperature of 0 ° degrees C and pressure of 800 hPa, to account for the high altitude of the station.

The model simulations at Hedo are in good agreement with the mean values for the three pollutants. Except for the *ACESS run* calculation of SO_2 concentrations, which probably is related to lower *ACESS* emission at the island. As mentioned earlier, is the island not surrounded by other high emission sources in the vicinity, and the concentrations are mainly affected by the

emission input and long-range transport. The *Original run* has calculated higher concentration, reflecting the effect of higher emission input, and the *ACESS* emission released at higher levels being more sensitive to long-range transport.
The correlations are low for both SO_2 and NO_2 concentrations at Hedo. The site is situated at an small island, and with such grid resolution the model has difficulties capturing the variations. Hedo has a large period with no observations of NO_2 concentrations, from May to November, which makes the basis of comparison poorer. However, Figure 5.11 shows the model results to be in good agreement with observational values for the period with measurements.

Happo shows some of the same peaks in observations of SO_2 concentrations as seen in the rural site Ijira (Figure 5.9). They are both situated on the island Honshu in Japan, and the southerly winds in this period can have the same effect, as described for Ijira. The industrial area south of the site is assumed to be the reason for the high SO_2 concentration peaks. The model does not reproduce these peaks in the SO_2 concentration.

The O_3 concentration in Hedo and Happo are considerably higher than for the urban and rural sites, especially Happo with a yearly mean value of 53.29 ppb. The sites are sensitive to long-range transport, and the NO-titration is not as important far from large emission sources. Happo is situated at high altitudes and is affected by winds transporting O_3, and also influenced by higher O_3 levels in the free troposphere.
The temporal correlation of O_3 concentrations at Hedo is good. Happo has not reproduced the seasonal variations of O_3 concentrations in either of the model results, the higher values in spring is not captured making correlation low. The global EMEP model has no convection scheme, which can effect the O_3 production, since precursors like NO_x and NMVOC are emitted mostly at the surface.

To summarize the global EMEP model performance with two different emission inventories in Asia when comparing with observations;

- The *ACESS run* shows better temporal correlations with observations for all pollutants; SO_2, NO_2 and O_3.
- Both model results show in general an underestimation of the SO_2 and NO_2 mean concentrations over Asia.
- The global EMEP model shows better skills in the calculations O_3 concentrations.
- The global EMEP model shows better skills in modelling the concentrations in rural and remote sites, as expected with such coarse grid resolution.
- The temporal correlations with observations are lower over Asia than over Europe, reflecting the coarser resolution, no seasonal variation in emissions and the scarce observational data in Asia.
- The *ACESS run* has generally not improved the simulation of mean concentrations, which can be related to the representativeness of remote sites only situated in Japan.

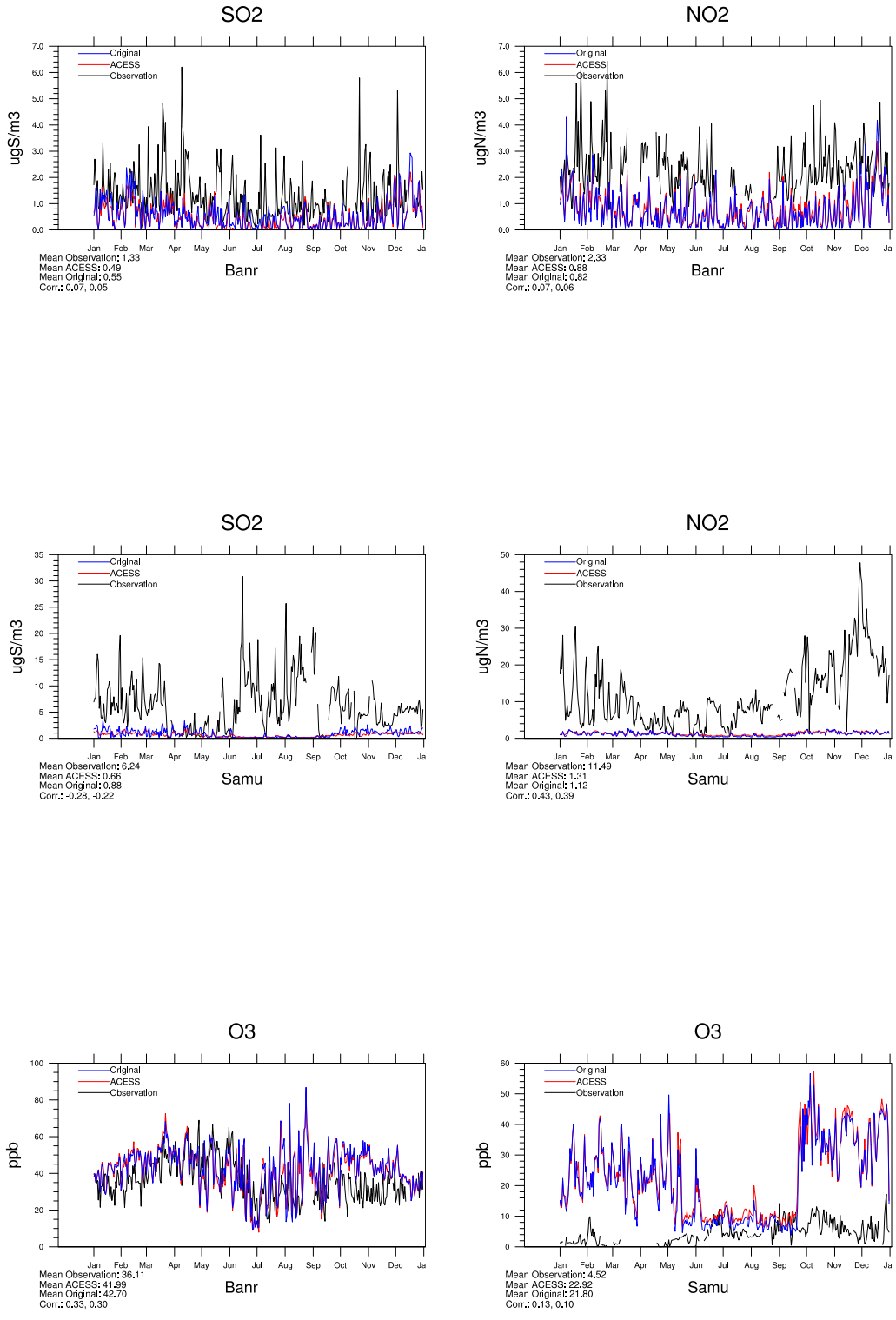

Figure 5.9: Time series of observations and model calculations of SO_2, NO_2 and O_3 in urban sites in 2001. The top panel show time series for Banryu, in the middle the site Samutprakarn is shown. And in the lower panel O_3 concentrations for the two sites are presented.

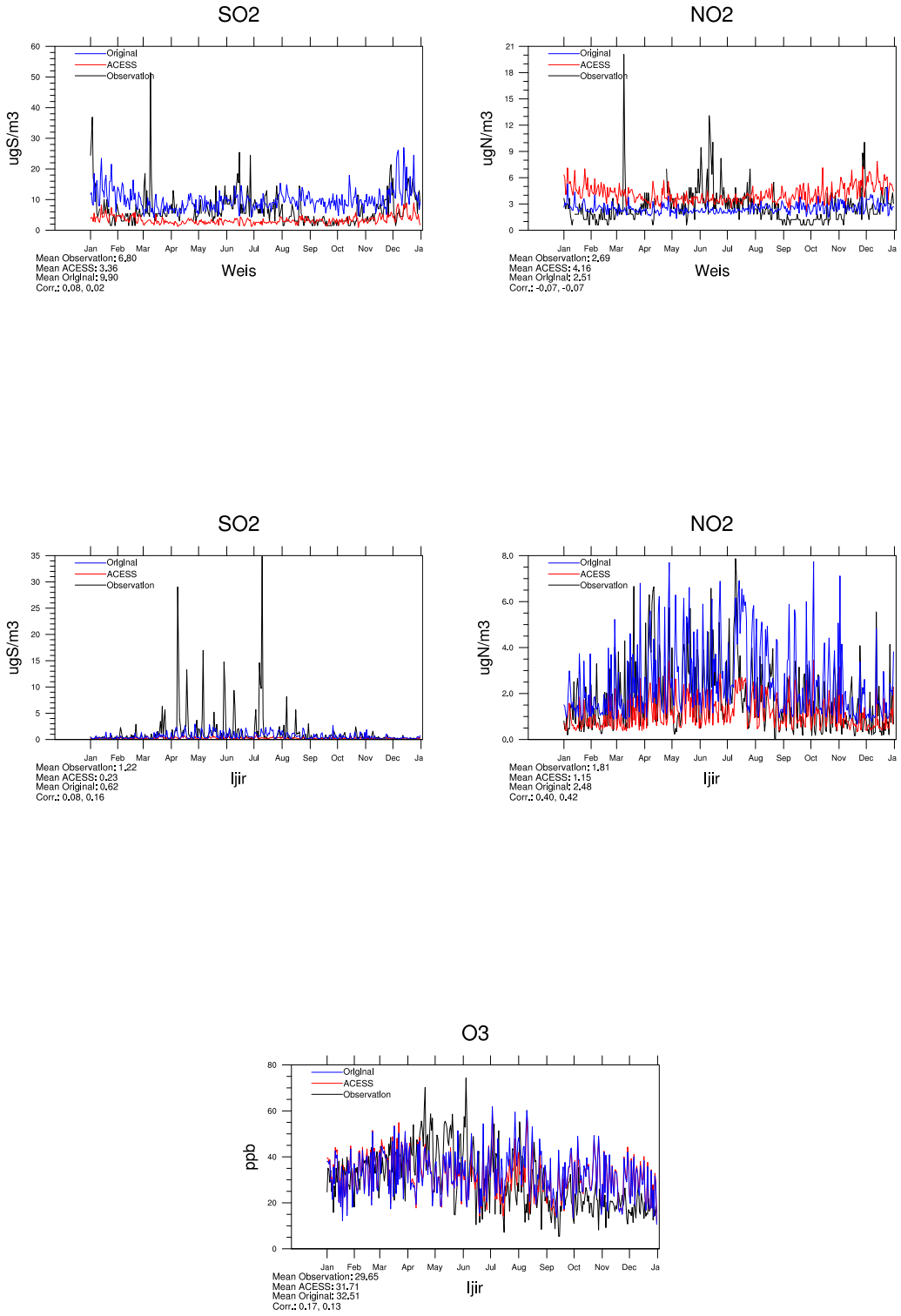

Figure 5.10: Time series of observations and model calculations of SO_2, NO_2 and O_3 in rural sites in 2001. The top panel show time series for Weishuiyuan, in the middle the site Ijira is shown. And in the lower panel O_3 concentrations for Ijira are presented.

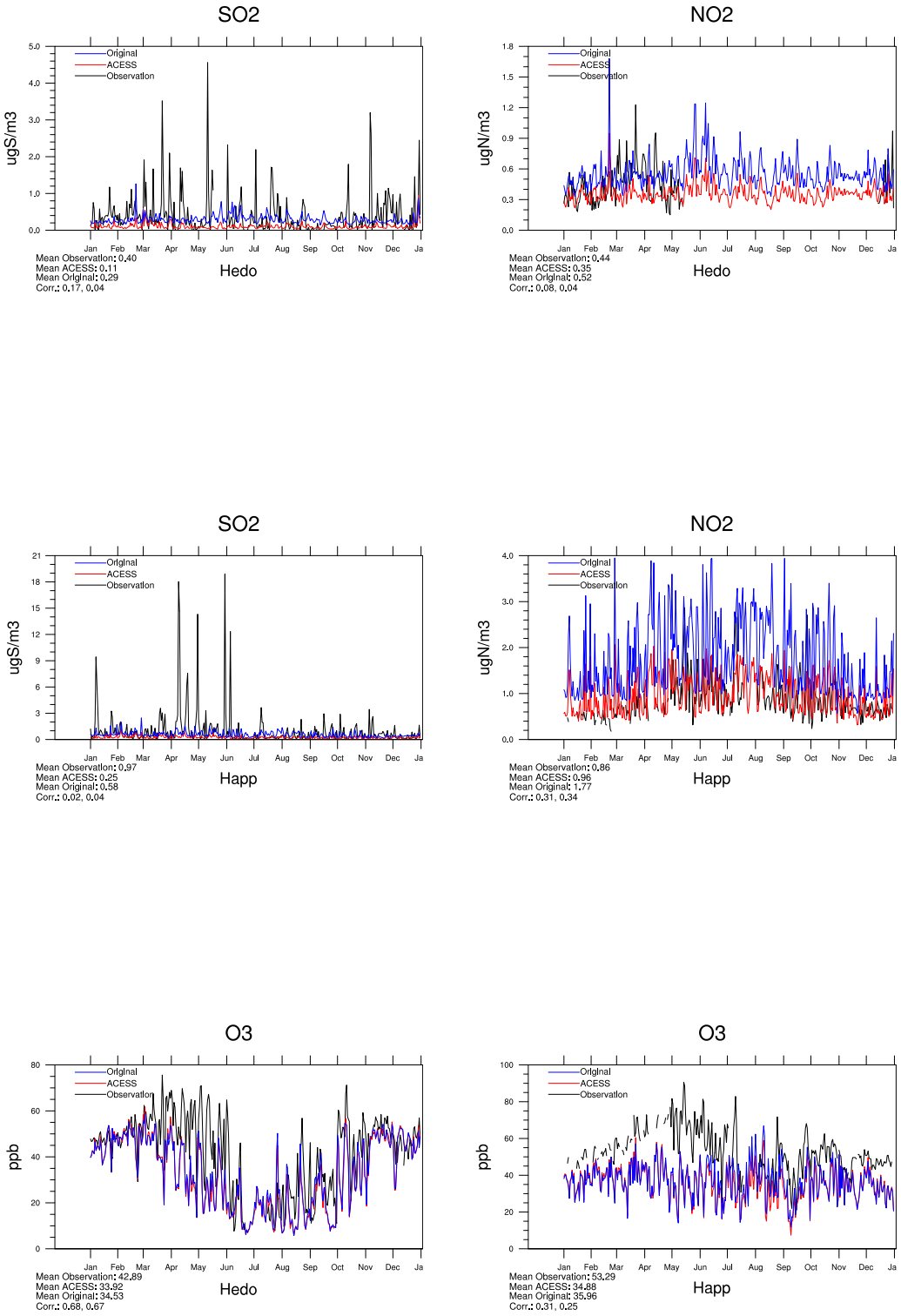

Figure 5.11: Time series of observations and model calculations of SO_2, NO_2 and O_3 in rural sites in 2001. The top panel show time series for Hedo, in the middle the site Happo is shown. And in the lower panel O_3 concentrations for the two sites are presented.

5.3 Comparison with other model results (MISC-II)

An intercomparison study of chemical transport models in East Asia was conducted by Carmichael et al. (2002), MICS-I, and an expanded version in 2003, MICS-II, (Carmichael et al., 2007). The study included nine regional models, and simulations were made over four different periods, including three different seasons over two years; March, July and December in 2001, and March in 2002. Eight models were compared in studies of deposition of sulfur and nitrogen compounds and O_3 (Han et al., 2007). The performance of these models is here compared with the performance of the global EMEP model.
The regional models in MICS-II have different grid-size, from 36 km to $0,5\,^\circ$, while the global EMEP model uses a coarser grid resolution of $1\,^\circ$ x $1\,^\circ$. For anthropogenic emissions the MICS models used TRACE-P inventory (Streets et al., 2003). In chapter 4 the emission totals from TRACE-P (Streets et al., 2003) were compared with the *Original* and the *ACESS* emission totals used in the global EMEP model, without finding large differences. For the MICS-II study, the emissions were modified to reflect the four periods studied. This has not been done in the emission inventory in the global EMEP model. For more information about details of the models included in the MICS model study, see Han et al. (2007). The different models were separated by numbers; from M1 to M8.

This section presents the comparison of the performance of the eight MICS models compared with the performance of the global EMEP model for March, July and December 2001. Note that MICS-II includes comparison in more stations than investigated in this thesis, namely Malaysia(24, 25), Mongolia(26, 27), Philippines(28, 29), Russia(33-36) and Vietnam(42, 43). These sites are not discussed here. The sites included are described in chapter 3.

Monthly variation in EANET sites

SO_2 and NO_2

The comparison of the model calculations and the observed monthly mean values for SO_2 and NO_2 concentrations done in the MICS-II study, and for the global EMEP model, are presented in Figure 5.12. An approximation of the EMS (Ensemble Mean Statistics) from MICS-II is also included. Note that the EMS MICS-II line is reproduced as an approximation and does not contain the actual numbers. The line is included to provide an image of how the global EMEP model performs compared to the mean of the MICS model results. In addition, it is important to investigate the variability of the regional model results from EMS in the different sites and months, as indicated in Figure 5.12.
The MICS-II study presented the calculations and measurements of mean concentrations in ppb, with a logarithmic scale. The same presentation was adopted for the observations and global EMEP model results from two model runs conducted in this thesis. The label with the different models presented in figure 5.12 is also valid for the comparison for O_3.

According to Carmichael et al. (2007), the models in the MICS study generally showed good skills in simulating the spatial variability, reflecting the location and intensity of the emissions, for instance the higher levels over China, and more moderate levels in Japan. This is also well simulated by the global EMEP model.
According to Han et al. (2007), the models in MICS-II generally overpredict the concentrations of SO_2, especially in the Chinese rural sites 2 (Jinyunshan) and 4 (Weishuiyuan), the urban site 22 (Ijira), in Japan, and the urban sites in Thailand. Carmichael et al. (2007) suggested the

overprediction in 4 (Weishuiyuan) and 22 (Ijira) to be related to the coarse resolution of the regional models and their inability to distinguish the gradient for rural sites possibly located near grid cells with large sulfur sources. The global EMEP model underestimates the concentrations in these sites as well, most likely caused by the coarse grid resolution. The global EMEP model underestimates in general SO_2 concentration, especially in July. However since the global EMEP model has an even coarser resolution than the models in MICS-II, with grid size of 1° x 1°, and no seasonal variations in the emission inventories, this underestimation was as expected.

NO_2 concentrations are generally underestimated in the global EMEP model, especially in the urban sites in China and Thailand; 6 (Hongwen), 37 (Bangkok) and 38 (Samutprakarn), and the remote sites in Japan; 14 (Rishiri), 15 (Tappi) and 17 (Sado). The underprediction in the urban sites is also seen in the MICS models. The models in MICS-II have somewhat similar underestimation, especially in 14 (Rishiri) in March and December. The better MICS model results in July, can be a consequence of the emissions modified to reflect the time periods in the MICS-II study. The remote site Happo in higher altitudes is generally overestimated in the MICS-II study, while the global EMEP model, and especially in the *ACESS run*, shows good skills in reproducing the NO_2 concentrations.

In general, the global EMEP model simulates SO_2 and NO_2 concentrations in good agreement with the regional models included in the MICS-II model study. Compared to some models, especially M4, that generally underestimates, and M2, with general overestimation, the global EMEP model shows better skills in simulating the monthly means of SO_2 concentrations, despite its coarser resolution.

Note that comparing the model results by using logarithmic scale, which makes the real overestimation or underestimation unclear. According to Carmichael et al. (2007), the ensemble means in the MICS-II study are reasonably consistent with the observations. The global EMEP model does not show significant differences from the EMS in MICS-II, and in some sites the global EMEP model show even better skills than most of the models participating in MICS-II. However, it is still an important challenge to improve model simulations of SO_2 and NO_2 concentrations over Asia.

O_3

Figure 5.13 presents the observed and simulated monthly mean concentration of O_3 from eight models participating in MICS-II, and the observations compared with simulations of the global EMEP model. The figures of the EMEP model calculations also include an approximation of the EMS from MICS-II. O_3 show less deviations of the model results from the measurements indicating a better general performance of the models for O_3. The scales are here given in a linear scale.
The global EMEP model is in good agreement with the EMS of the MICS-II model study, and also shows good skills in predicting the seasonal variation in the sites. For instance, like most models in MICS-II, the global EMEP model reproduces the lower values in 21 (Hedo) in July and higher concentration during winter/spring when the winter monsoon brings continental pollution. However, the high concentration in the high altitude site Happo is generally underestimated in the MICS-II study, as well as in the global EMEP model. The reason suggested by Carmichael et al. (2007), is associated with the models vertical resolution and mixing of O_3 from the upper troposphere. That can also apply to the global EMEP model.
Different models in the MICS-II study show underestimation, like M2 and M4, or overestima-

tion, M1 and M5, of the O_3 concentrations in certain months. The global EMEP model does not show any general overestimation or underestimation of this kind, and the model simulations are in good agreement with the observations of O_3.

To summarize the global EMEP model performance compared with other model results, MICS-II, in Asia:

- The performance of the global EMEP model is in the same range as the ensemble of the MICS models for all components analysed; SO_2, NO_2 and O_3. This despite the coarser resolution.
- The challenges to improve the performance of the global EMEP model in Asia as derived from the comparison with observations in this section, seem to be common challenges for regional models that participated in the MICS-II model study.

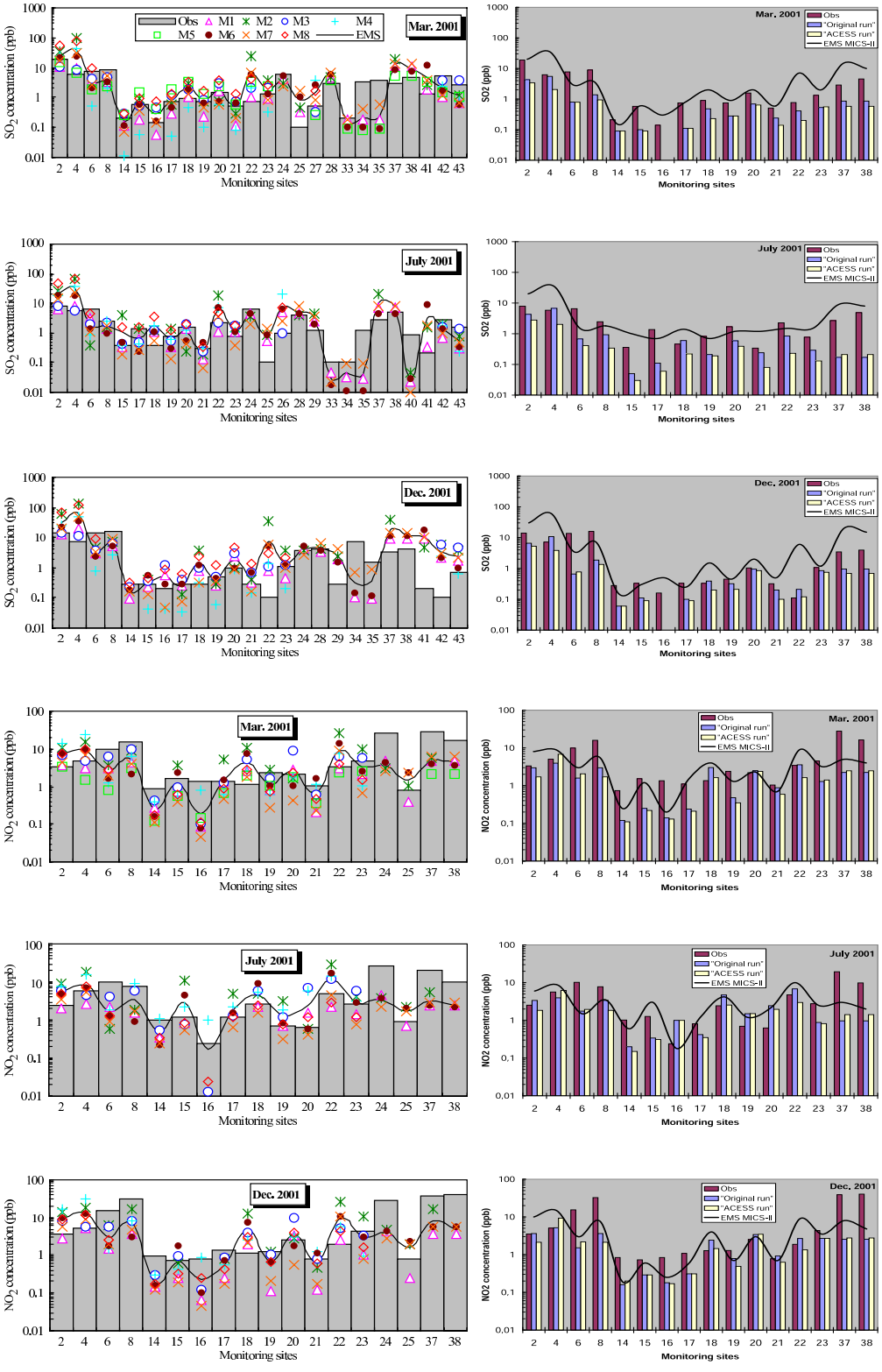

Figure 5.12: Comparison of monthly average concentrations for SO_2 and NO_2 in MICS-II and the global EMEP model in March, July and December. SO_2 concentrations are given in the first six figures and NO_2 concentrations in the six following plots. The figures to the right are values from this thesis and the figures to the left are taken from MICS-II study, Carmichael et al. (2007).

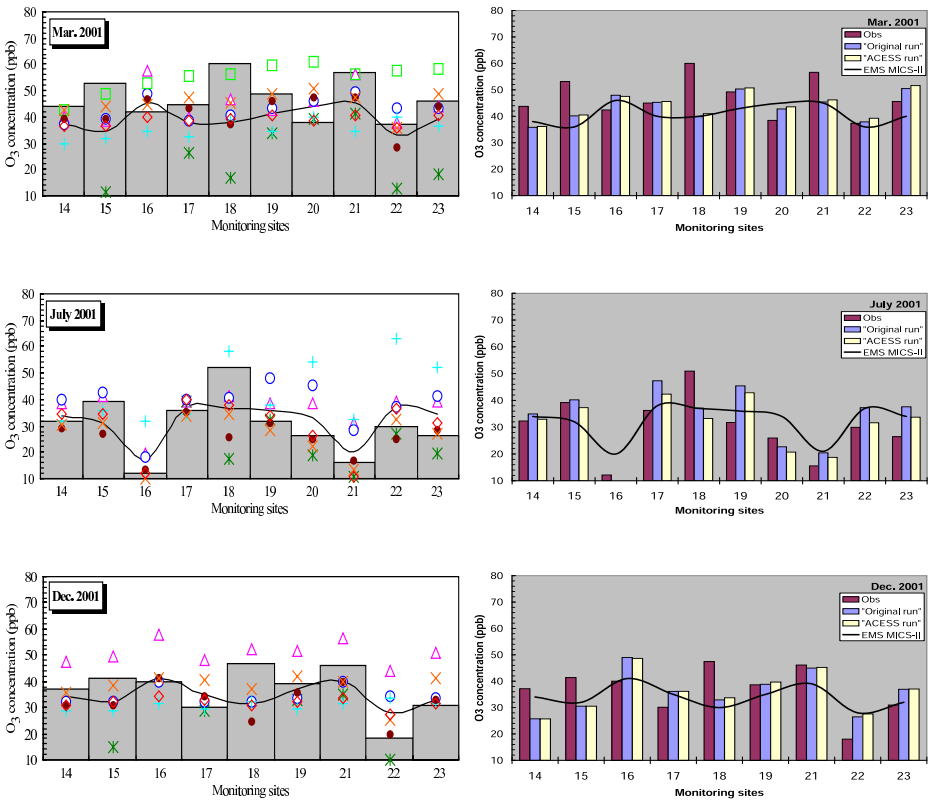

Figure 5.13: Comparison of monthly average concentrations for O_3 in MICS-II and the global EMEP model in March, July and December. The figures to the right contain values from this thesis and the plots to the left are taken from MICS-II study, Carmichael et al. (2007).

Chapter 6

Discussion

The performance of the global EMEP model has in this thesis for the first time been evaluated in detail over Asia. The model results have been analysed for SO_2, NO_2 and O_3, by comparison with observations in urban, rural and remote sites at the EANET network, for the year 2001. In addition, the global EMEP model results have been compared against other modelling results in Asia from the MICS-II study. In order to better understand the effects of emissions on model results, the model was run twice for the year 2001 with different emission inventories. The model results show a great deal of uncertainties over Asia, and the discussion in this chapter is on the model performance and possible improvements.

6.1 Analysis of model performance

The global EMEP model shows in general an underestimation of the air concentrations of SO_2 and NO_2 when compared with observations in Asia. However, there is a clear difference in the model performance for urban, rural and remote sites. The model results show better agreement with observations for rural and remote sites, for both SO_2 and NO_2 concentrations. Compared to the performance of European model simulation, from the regional EMEP model, the global EMEP model show high underestimation of SO_2 and NO_2 concentrations in Asia.

The model results were also compared with other regional model performances from the model study MICS-II, (Carmichael et al., 2007), in Asia, and found to be the same range for SO_2, NO_2 and O_3 concentrations. However the presentations of the comparison made against observation in the model study for SO_2 and NO_2 were given in logarithmic scale. This presentation gives a indication that the models performs better then if presented in linear scale. The comparison shows that the challenges to improve the global EMEP model over Asia are also valid for other regional models in the area.

The global model was run with two different emission inventories for Asia, to better understand effects of emissions on model results. Differences in the emission inventories were especially related to the allocation of the emissions in source sectors. The *Original* emission contained errors since the emissions were mainly distributed in S7, road traffic. The new *ACESS* emissions showed a more detailed distribution in source sectors, with more emission released at higher altitudes. The change in emissions implied in general no improvement in the simulations of the surface air concentrations of SO_2 and NO_2. This was possibly related to the representativeness of remote sites over Japan, where the adjustment of the ACESS emissions from 2006 to 2000 resulted in too low emissions in Japan. However, the correlation of the model results with ob-

servations showed an improvement in the *ACESS run*, with a more adequate emission sector distribution. SO_2 had an increase in the mean temporal correlation by 0.016, for NO_2 the value was calculated to 0.021, and for O_3 an increase of 0.019.
Analysing the differences between the two model runs at higher vertical levels showed significant larger effect on long-range transport in the model results where the pollutants were emitted at higher levels. Especially for SO_2, where differences in the model results could account for up to 20% reaching as far as North-America. Over the boundary layer, the effect of more substantial long-range transport in the *ACESS run*, was seen for all pollutants analysed. These effects are related to the vertical distribution of emissions, and indicates the distribution in source sectors to be highly relevant for understanding the impact of Asian pollution on other continents.
For both model experiments the performance of the global EMEP model in Asia is generally poorer than over Europe.

6.2 Representativeness of observations

The observations used for evaluation of model results in this thesis are from the EANET network, which started their monitoring activities in 2001. Observations from sites in Japan, China and Thailand are used for comparison with model results.

Spatial representativeness of observations

The spatial distribution of the available observational data was highly biased in Japan, while the rest of Asia had a scarce selection of sites, with only four sites in the largest country, China, and two in Thailand. The lack of spatial representativeness hampers the conclusions drawn from the comparison with observations. Areas highly polluted in the northeast of China, especially around Beijing, where also large differences between the model runs occurred, were unfortunately not well represented with observations.

In the model study MICS-II, (Carmichael et al., 2007), the model results were also compared with observations from EANET for the year 2001. However, the model study included observations from Malaysia, Mongolia, Philippines, Russia and Vietnam. Unfortunately these observations were not available for this thesis.

Further evaluation of model performance over Asia should include, if possible, a larger number of observation stations.

Errors in measurements

The EANET network started their monitoring activities in 2001 and it is possible that, especially in this initial phase, errors with the measurements could occur. For instance, the O_3 measurements at Samutprakarn, with concentrations under 10 ppb throughout the year, are questionable. The observations can contain errors and this must be taken into consideration.

Comparison with observations in urban, rural and remote sites

The global EMEP model has a grid resolution of 1° x 1°, and the concentrations simulated in the model are averages of the area included in the grid box of about 110 x 110 km^2. This grid area can include emission sources; and urban, rural and remote areas, all in one grid. When comparing the models simulation with observations, the grid resolution and locations of the sites

must be considered. The sites are classified in urban, rural and remote, according to the distance from large emission sources.
The model is most likely not able to capture the high concentrations in an urban site, situated close to high emission sources. The locations of the sites are therefore an important factor to consider when interpreting model performance. The expectations to the model performance regarding urban, rural and remote sites were discussed more in details in the previous chapter. The global EMEP model clearly show better skills in simulating concentrations at rural and remote sites. It was expected that the global EMEP model performance showed even better agreement at remote sites. However, all the remote sites with observations available, was situated in Japan. And this made a poor basis of comparison for the global model performance in remote sites in general.

6.3 Grid resolution

The coarse grid resolution in the global EMEP model, 1° x 1°, are highly relevant when evaluating the model results.

Input data

The input data in the model; meteorology, land-use and emission data are all given in the same resolution. Inside a grid box of 1° x 1° there are many differences, in emission sources, their size and location, land cover, and also the meteorological conditions. The model calculates an average of the processes and variables in the grid, so the variations inside the grid are not well reproduced.

Grid resolution affecting O_3 and NO_x model results

The sensitivity of the model grid resolution for O_3 results has been a subject of interest in different articles. Caarey Jang et al. (1995)have investigated the difference in using grid resolution of 20, 40 and 80 kilometers. The conclusions made in Caarey Jang et al. (1995) were that the coarser model tends to underpredict O_3 maxima in the city downwind areas, in which the emissions of O_3 precursors were diluted, thereby producing less O_3; and tends to overpredict O_3 minima in intense NO_x emissions areas, because the NO titration effect of O_3 were underpredicted. Other model studies (Lin, 1988; Sillman et al., 1990) showed generally the same conclusions; in a coarser-grid model with an equal size of source area, it can be produced more O_3 than in a finer-grid model.
These conclusions justify also the performance of the global EMEP model. Overprediction of O_3 can take place in a area with intense NO_x emission. In the model runs, the sites close to large emission sources often had higher O_3 concentration then the observations. This is presented in Table 5.3, where the urban and rural sites overestimate the O_3 concentration. Table 5.2 presents an underestimation of NO_2 concentrations in the same sites, especially in the urban sites. The underestimation of NO_x concentrations in the global simulation seems to be related to underestimation of the NO titration effect of O_3, as indicated by Caarey Jang et al. (1995).

The global EMEP model performance over Asia is most likely to show better skills by running the model with a finer grid resolution. However, the regional models in the MICS-II model study (Carmichael et al., 2007) with resolution of either 36 km, 40.5 km, 45 km or 0.5°, also seem to have the same difficulties as the global EMEP model in Asia.

6.4 Uncertainties in the global EMEP model formulation in Asia

The global EMEP model is a chemical transport model based on the continuity equation. In general any CTM is a simplification of the real world, and the atmosphere is to complex to be able to recreate all the details of the different processes.
The global EMEP model is an extension of the regional EMEP model, and except for grid projecting and input data; meteorology, emissions and description of land cover, the models are the same. The regional EMEP model performs well over Europe, however it is possible that the extension to a global scale needs more adjustments in certain aspects, specially over Asia. Following is a discussion in order to understand why the performance of the model over Asia is poorer than over Europe.

Land-use and deposition in Asia

Land cover data, in the area outside Europe, is in the global EMEP model from MM5, the Fifth-Generation NCAR/Penn State Mesoscale Model. The land-use data from MM5 was interpolated to the 16 land-use types applied in the EMEP model. This interpolation is a simplification, considering that Asia has other land-use types than in Europe, and the values need to be verified. The EMEP land-use over Europe has been extensively validated for Europe, but not in other areas of the world. The land-use effects the deposition of pollutants, especially for SO_2 and NO_2. The deposition model has been calculated for vegetation types across Europe (Emberson et al., 2000; Tuovinen et al., 2001, 2004), and variables like the surface resistance are likely to differ in Asia.

Therefore it is recommended to validate the land-use types in Asia and other continents in further development of the global EMEP model.

Chemistry on dust particles

The global EMEP model uses the EMEP photochemistry, with a simplified treatment of particulate matter. There is a version of chemical scheme including aerosol dynamics and different natural particulate matter sources, like biomass burning and natural dust, but this version is not used here.

The fact that there is no natural dust or reactions on natural dust included in the global EMEP model, can be significant for the model results. For instance, the Gobi desert situated in Mongolia and China, impacts the level of particles in the sites in Asia. Dust storms, especially during spring in northern China, are frequently seen to produce a large amount of mineral dust. This can affect for instance biochemical processes over China (Zhang et al., 2009). A study of ground observations of dust aerosols in Beijing was conducted by Zhang et al. (2009), show that mass elements of particles increased in the times of dust storms and mainly had an origin in Gobi and deserts in regions of Mongolia ans northern China. Especially the elements Mg (magnesium), Si (silicon), Fe(iron), Al(aluminium) or Ti(titanium) are indicators of transport of dust, Cl can be a product of mixing with particles and anthropogenic emissions.
Wu and Okada (1994) claims that airborne crustal material reacts with HNO_3 (nitric acid). In this way the balance between HNO_3 and NH_3 is altered. This can again impacts the concentrations of SO_4 (sulfate), since HNO_3 and SO_4 both react with NH_3, see balances described in Simpson et al. (2003). Even if the order of the reactions is not clear, it is likely that the concentration of NH_3 will be affected. This again affects the dry deposition of SO_2, since resistance

variables for dry depositions of SO_2 vary with the amount of NH_3 (Simpson et al., 2003).
In addition, Li and Shao (2008) has results indicating that mineral particles in brown haze episodes were involved in atmospheric heterogeneous reactions with two or more acidic gases (e.g. NO_2, SO_2,HCl and HNO_3). This indicates that natural dust and reactions linked with for instance dust from the Gobi desert can affect the concentrations of SO_2 and NO_2.

For future applications over Asia it is recommended to implement aerosol dynamics and natural dust in the global model.

Convective scheme

As mentioned in chapter 2, does the EMEP model not include horizontal eddy diffusion and convection terms. This can be a limitation for both horizontal and vertical transport. The convective transport is treated as a part of the vertical exchange routine, with effective vertical diffusion coefficients (Jonson et al., 2007). This was sufficient for the regional model. But the a global model include areas like the equatorial regions, which are more affected by convective events.
Convection mainly caused by solar heating and is an effective process for vertical exchange of heat, mass and momentum in the atmosphere. The air near the surface, especially at lower latitudes, is warmed up by the sunlight, this makes the air density to decrease and creating convective instability. The process turns in to a motion of upward air, and there will be a vertical mixing. Convective processes are therefore important for transporting near-surface gases into the free troposphere, and it is done more rapidly than large scale motion. This can have an effect on for instance O_3 production, since precursors like NO_x and NMVOC often are released by the surface. If transported into the free troposphere, NO_x has a higher O_3 production rate per molecule than at the surface (Jonson et al., 2007).

However, the importance of convection has been taken into account, and the EMEP models convection parametrization is initiated and currently in progress.
This can justify the global EMEP model performance over Asia to some extent.

6.5 Emissions over Asia

The global EMEP model performance over Asia, when compared with surface observations, was only slightly improved with the new *ACESS* emission inventory. There still seems to be room for improvement on the Asian emissions. The emissions were adjusted from ACESS 2006 to ACESS 2000 by percentage differences given on ACESS webpage, (Streets and Zhang, 2008). However, these adjustments are not merely growth in emissions, but could also include improvements and corrections made to the original TRACE-P inventory from 2000, and also effects of replacing the TRACE-P inventory by local inventories several countries. The adjustments gave therefore emissions totals in the same range as in the *Original* emission inventory.

In addition, the adjustment factors used were based on the difference between ACESS 2000 to ACESS 2006 for the entire area, and without differencing in a spatial sense. For Japan these adjustments made the emissions in the *ACESS* inventory too low, since the increase of emissions in Japan, from 2000 to 2006, are much lower than for the rest of Asia, and then especially China. This can be a reason for some of the lower values in the concentrations of SO_2 and NO_2 in Japan in the *ACESS run.*
It is therefore recommended to further improve the emission data over Asia. The adjustment for

the ACESS 2006 emission inventory should include only increase in emissions and should differ in a spatial sense as well. It is also recommended to use seasonal variations in the emission data, and to improve the source sector distribution for all pollutants; NH_3 and PM as well.

Chapter 7

Conclusions and recommendations

In this thesis the global EMEP model has been evaluated over Asia for the first time in detail. The model results of SO_2, NO_2 and O_3 concentrations were analysed by comparison with observations and other model results. The validation of the model performance against observations distinguished especially between urban, rural and remote sites. The global model was run twice for the year 2001 with two emission inventories, to better understand the effects of emission data on model results.

The model results were compared with each other and with observations from the EANET network. The model results showed both a general underestimation of SO_2 and NO_2 concentrations in Asia, while for O_3 concentrations the model results were more consistent with measurements. However, there were a difference in the model performance at urban, rural and remote sites. The global EMEP model shows better simulations in rural and remote sites. However, compared to the performance of European model simulation from the regional EMEP model, the global EMEP model show high underestimations of SO_2 and NO_2 concentrations in Asia. However all the remote sites with available observations were situated in Japan, which gave a poor basis of comparison.

The two different emission inventories used in the global EMEP model, the *Original* and the *ACESS* emissions, were evaluated over Asia. The emission totals of the four main pollutants; SO_2, NO_x, CO and NMVOC, were validated with other emission estimates for the region, and found to be of same order of magnitude as emissions in scientific literature (Cofala et al., 2007; Ohara et al., 2007; Streets et al., 2003). The main differences between the emission inventories were the allocation of emissions in source sectors. The *Original* emissions showed to be placed mainly in S7, road traffic, where the pollutants are emitted at the lowest layer of the atmosphere. The new *ACESS* emissions showed more detailed source sector distribution, with emissions in the four sectors, S1; combustion in energy and transformation industries, S2; non-industrial combustion plants, S3; combustion in manufacturing industry, and S7; road transport. The sector distribution in the *ACESS* emissions gave a higher vertical distribution of the emissions than in the *Original* emission inventory, since especially S1 and S3 emits the pollutants at higher levels.

When comparing the two model results with observations, the correlations for all pollutants analysed were slightly increased in the *ACESS run*. SO_2 in the *Original run* simulated a mean temporal correlation of 0.123 and for the *ACESS run* the temporal correlation was 0.139. The mean correlations for NO_2 were calculated to 0.163 and 0.185 for the *Original run* and the *ACESS run*, respectively. Also for O_3 the correlation increased from 0.429 in the *Original run*

to 0.448 in the *ACESS run.* The correlation show a slight improvement by distributing the emissions in different source sectors.
The *ACESS run* with pollutants distributed more in higher levels, showed a significant increase in long-range transport. Especially for SO_2, with air concentrations reaching as far as North-America, accounting for up to 20%, at ~680 meters height. Also at surface level was the long-range transport of SO_2 obvious, with over 20% increase. Over the boundary layer, at ~2890 height, the effect of more long-range transport in the *ACESS run* was seen for all three pollutants analysed.
However, the *ACESS run* did generally not improvement in the model simulations of the surface air concentrations of SO_2 and NO_2. Which can be related to the representativeness of remote sites over Japan, and the adjustment of the *ACESS* emissions from 2006 to 2000 resulting in too low emissions in Japan.

This thesis included a validation of the model results in the global EMEP model over Asia with other model results in this region. The MICS-II model study, including eight regional models, were conducted in the area (Carmichael et al., 2007). The model study provided a benchmark for other chemical transport models performance in the area. The comparison with the regional models implied the model results from the global EMEP model generally to be in the same range as the regional models participating.

However the underestimation in the model results are substantial and recommendations for further improvements are included.
The grid resolution of the global EMEP model is coarse, and by using a finer resolution it is expected to improve the performance of the model in the area over Asia. Therefore, the use of the global model in a resolution of 0.5° x 0.5° are recommended in further studies, especially as the ACESS emission are already available in this resolution.
The emission data over Asia is also recommended to be further improved. The adjustment factors from 2006 to 2000 should include only growth in emissions over the period, and the spatial distribution should be considered. It is also recommended to apply a seasonal variation in the emissions. These recommendations can improve the global model simulations over Japan especially.
In future applications the global EMEP model it is recommended to run the model with aerosol modes and includes sources of particulate matter, especially biomass burning and natural dust.
The initiated work to develop the convection parametrization in the EMEP model will also contribute to improve the performance of the model results, specially for O_3.
Land-use types applied in the global EMEP model are evaluated for Europe but not for Asia, and can affect processes like dry deposition significantly. Therefore the last recommendation is that the land-use types used in Asia and other continents are thoroughly validated for further use in the global EMEP model.

Bibliography

Acid Deposition and Monitoring Network in East Asia (2009). EANET. Accessed March 2009. $http://www.eanet.cc/$.

Andersson-Sköld, Y. and D. Simpson (2001). Secondary organic aerosol formation in Northern Europe: a model study. *Journal of Geophysical research 106*(D7), 7357–7374.

Auvray, M. and I. Bey (2005). Long-range transport to Europe: Seasonal variations and implications for the European ozone budget. *Journal of Geophysical Research 10*.

Bey, I., D. J. Jacob, J. A. Logan, and R. M. Yantosca (2001, October). Asian chemical outflow to the Pacific in spring: Origins, pathways and budgets. *Journal of Geophysical Research 106*, 23097–23113.

Caarey Jang, J.-C., H. E. Jeffries, D. Byun, and J. E. Pleim (1995). Sensitivity of Ozone to Model Grid Resolution - I. Application of High-Resolution Regional Acid Deposition Model. *Atmospheric Environment*, 3085–3100.

Cancer Research UK, C. R. U. (2009, March). Lung cancer risks and causes. Accessed March 2009. $http://www.cancerhelp.org.uk/help/$.

Carmichael, G. R., G. Calori, H. Hayami, I. Uno, S. Y. Cho, M. Engardt, S. B. Kim, Y. Ichikawa, Y. Ikeda, J. H. Woo, H. Ueda, and M. Amann (2002). The MICS-Asia study: model intercomparison of long-range transport and sulfur deposition in East Asia. *Atmospheric Environment 36*, 175–199.

Carmichael, G. R., T. Sakurai, D. Streets, Y. Hozumi, H. Ueda, S. U. Park, C. Fung, Z. Han, M. Kajino, M. Engardt, C. Bennet, H. Hayami, K. Sartelet, T. Holloway, Z. Wang, A. Kannari, J. Fu, K. Matsuda, N. Thingboonchoo, and M. Amann (2007). MICS-II: The model intercomparison study for Asia phase II methodology and overview of findings. *Atmospheric Environment*, 3468 – 3490.

Cofala, J., M. Amann, Z. Klimont, K. Kupiainen, and L. Höglund-Isaksson (2007). Scenarios of local anthropogenic emissions of air pollutants and methane until 2030. *Atmospheric Environment* (41), 8486–8499.

Collins, W. J., D. S. Stevenson, C. E. Johnson, and R. G. Derwent (2000). The European regional ozone distribution and its links with the global scale for the years 1992 and 2015. *Atmospheric Environment* (34), 255–267.

Commission on Geosciences, C. (1999). *Ozone-Forming Potential of Reformulated Gasoline*. National Academy Press, Washington, D.C. Accessed May 2009. $http://www.nap.edu/catalog.php?record_id = 9461$.

Cooper, R. O. and D. D. Parrish (2004). Air Pollution Export from and Import to North America: Experimental Evidence. In A. Stohl (Ed.), *Intercontinental Transport of Air Pollution*, pp. 41–67. Springer-Verlag Berlin Heidelberg New York.

Derwent, R. G., D. S. Stevenson, R. M. Doherty, W. J. Collins, and M. G. Sanderson (2008). How is surface ozone in Europe linked to Asian and North American NO_x emissions? *Atmospheric Environment* (42), 7412–7422.

Dunlop, S. (2001). *Oxford Dictionary of Weather*. Oxford University Press.

EDGAR, M. N. E. A. A. (2005). Emission Database for Global Atmospheric Research, EDGAR. Accessed March 2009. *http://www.mnp.nl/edgar/*.

Emberson, L., M. R. Ashmore, H. M. Cambridge, D. Simpson, and J. P. Tuovinen (2000). Modelling stomatial ozone flux across Europe. *Environmental Pollution*, 403–414.

EMEP (2009). Convention on Long-Range Transboundary Air Pollution. Accessed March 2009. *http://www.emep.int/*.

EMEP/CORINAIR (2000). EMEP/CORINAIR Atmospheric Emission Inventory Guidebook, Second Edition.

ENER-G UK, U. (2009). Efficient Energy Solutions, Glossary of Terms. Accessed March 2009. *http://www.energ.co.uk/energy_glossary*.

Environmental Protection Agency, U. S. (2008, April). Six Common Air Pollutants. Accessed March 2009. *http://www.epa.gov/air/urbanair/*.

Fagerli, H. and W. Aas (2008). Trends of nitrogen in air and precipitation: Model results and observations at EMEP sites in Europe, 1980-2003. *Environmental Pollution*, 448–461.

Fagerli, H., D. Simpson, S. Tsyro, S. Solberg, and W. Aas (2003). Transboundary Acidification, Eutrophication and Ground Level Ozone. Part II. Unified EMEP Model Performance. Technical report, Norwegian Meteorological Institute.

Han, Z., T. Sakurai, H. Ueda, G. R. Carmichael, D. Streets, H. Hayami, Z. Wang, T. Holloway, M. Engardt, Y. Hozumi, S. U. Park, M. Kajino, K. Sartelet, C. Fung, C. Bennet, N. Thingboonchoo, Y. Tang, A. Chang, K. Matsuda, and M. Amann (2007). MICS-II: Model intercomparison and evaluation of ozone and relevant species. *Atmospheric Environment 42*, 3491 – 3509.

Informasjonsgruppen Mot Sur Nedbør (1987). *STOPPSur Nedbør*. Euro Trykk.

Jacob, D. (January 1999). *Introduction to Atmospheric Chemistry*. Princeton University Press, Princeton, New Jersey.

Jonson, J. E., D. Simpson, H. Fagerli, and S. Solberg (2006). Can we explain the trends in European ozone levels? *Atmos. Chem. Phys.*, 51–66.

Jonson, J. E., J. K. Sundet, and L. Tarrasón (2001). Model calculations of present and future levels of ozone and ozone precursors with a global and a regional model. *Atmospheric environment*, 525–537.

Jonson, J. E., L. Tarrasón, P. Wind, M. Gauss, S. S. Valiyaveetil, S. Tsyro, H. Kein, I. S. Isaksen, and A. Benedictow (2007). First evaluation of the performance og the global EM EP model and comparison with global OsloCTM2 model. Technical Report 2, EMEP msc-w and uio.

Jonson, J. E., P. Wind, M. Gauss, S. Tsyro, S. O. A., H. Klein, I. S. A. Isaksen, and L. Tarrasón (2006, July). First results from the hemispheric EMEP model and comparison with the global Oslo CTM2 model. Technical Report 2, EMEP msc-w and uio.

Li, J., Z. Wang, H. Akimoto, C. Gao, and P. Pochanart (2007). Modeling study of ozone seasonal cycle in lower troposphere over East Asia. *Journal of Geophysical Research 112*.

Li, W. J. and L. Y. Shao (2008). Observation of nitrate coatings on atmospheric mineral dust particles. *Atmospheric Chemistry and Physics Discussions*.

Lin, X. (1988). On the nonlinearity of the troposphere ozone production. *J.geophys.*, 15,879–15,888.

Maes, J., J. Vliegen, K. Van de Vel, S. Janssen, F. Deutsch, and K. De Ridder (2009). Spatial surrogates for the disaggregation of CORINAIR emission inventories. *Atmospheric Environment 43*, 1246–1254.

Nakicenovic, N., J. Alcamo, G. Davis, B. de Vries, J. Fenhann, S. Gaffin, K. Gregory, A. Grüler, T. Y. Jung, T. Kram, E. Lebre La Rovere, L. Michaelis, S. Mori, T. Morita, W. Pepper, H. Pitcher, L. Price, K. Riahi, A. Roehrl, H.-H. Rogner, A. Sankovski, M. Schlesinger, P. Shukla, S. Smith, R. Swart, S. van Rooijen, N. Victor, and Z. Dadi (2000, November). Special Report on Emissions Scenarios. Technical report, Intergovernmental Panel on Climate Change, IPCC.

Network Center for EANET, E. (2002, November). Data Raport on the Acid Deposition in the East Asian Region. Technical report, EANET. Available at web-page $http://www.eanet.cc/product/datarep/datarep01/datarep01\_intro.pdf$.

Ohara, Y., H. Akimoto, J. Kurokawa, N. Horii, K. Yamaji, X. Yan, and T. Hayasaka (2007). An Asian emission inventory of anthropogenic emission sources for the period 1980-2020. *Atmospheric Chemistry and Physics*, 4419 – 4444.

Pochanart, P., O. Wild, and H. Akimoto (2004). Air Pollution Import to and Export from East Asia. In A. Stohl (Ed.), *Intercontinental Transport of Air Pollution*, pp. 99–130. Springer-Verlag Berlin Heidelberg New York.

Sase, H., T. Ohizumi, S. Nakayama, L. C. Peng, and H. Ueda. Acid deposition, soil pollution and plant growth: current status and future forest ecosystems. International Plantation Industry Conference and Exhibition 2008.

Seinfeld J.H. and Pandis S.N. (1998). *Atmospheric Chemistry and Physics*. Wiley-Interscience.

Sillman, S. (1999). The relation between ozone, NO_x and hydrocarbons in urban and polluted rural enviroments. *Atmospheric Environment* (33), 1821–1845.

Sillman, S., J. A. Logan, and S. C. Wofsy (1990). The sensitivity of ozone to noitrogen oxides and hydrocarbons in regional ozone episodes. *J. geophys.*, 1835–1851.

Sillmann, S. (2004). Overview: Tropospheric ozone, smog and ozone - NO_2 -VOC sensitivity. Acccessed March 2009. $http://www-personal.engin.umich.edu/sillman$.

Simpson, D., H. Fagerli, S. Hellsten, J. C. Knulst, and O. Westling (2006). Comparison of modelled and monitored deposition fluxes of sulphur and nitrogen to IPC-forest sites in Europe. *Biogeosciences*, 337–335.

Simpson, D., H. Fagerli, J. E. Jonson, S. Tsyro, and J.-P. Tuovinen (2003). Transboundary Acidification, Eutrophication and Ground Level Ozone in Europe, PART I, Unified EMEP Model Description. Technical Report 1, Norwegian Meteorological Institute.

Smith, S., R. Andres, E. Conception, and J. Lurz (2004, January). Historical Sulfur Dioxide Emissions 1850-2000: Methods and Results. U. S. Department of Energy. Joint Global Change Research Institute.

Stevenson, D., J. F. Dentener, M. G. Schultz, K. Ellingsen, T. P. C. van Noije, O. Wild, G. Zeng, M. Amann, C. S. Atherton, N. Bell, D. J. Bergmann, I. Bey, T. Butler, J. Cofala, W. J. Collins, R. G. Derwent, R. M. Doherty, J. Drevet and, E. H. J., A. M. Fiore, M. Gauss, D. A. Hauglustaine, L. V. Horowitz, I. S. A. Isaksen, M. C. Krol, J.-F. Lamarque, M. G. Lawrence, V. Montanaro, J. F. Müller, G. Pitari, M. J. Prather, J. A. Pyle, S. Rast, J. M. Rodriguez, M. G. Sanderson, N. H. Savage, D. T. Shindell, S. E. Strahan, K. Sudo, and S. Szopa1 (2006). Multimodel ensemble simulations of present-day and near-future tropospheric ozone. *Journal of Geo*.

Streets, D., T. Bond, G. Carmichael, S. Fernandes, Q. Fu, D. He, Z. Klimont, S. Nelson, N. Tsai, M. Wang, J.-H. Woo, and K. Yarber (2003). An inventory of gaseous aerosol emissions in asia in the year 2000. *Journal of Geophysical Research*.

Streets, D. and Q. Zhang (2008). Emission Data. Accessed September 2008. *http* : *//www.cgrer.uiowa.edu/EMISSION_DATA_new/index*_16.*html*.

Tarrasón, L., A. Gusev, O. Travnikov, V. Sokovych, K. Tørseth, M. Gauss, J. E. Jonson, A. Nyìri, and P. Simpson, David Wind (1/2008). Towards the development of a common EMEP global modelig framework. Technical report, MSC-E, CCC and MSC-W.

Tropospheric Emission Monitoring Internet Service The Netherlands, T. (2009). Sulfur dioxide. Accessed May 2009. *http* : *//www.temis.nl/products/so*2.*html*.

Tuovinen, J.-P., M. R. Ashmore, L. D. Emberson, and D. Simpson (2004). Testing and improving the EMEP ozone deposition module. *Atmospheric Environment*, 2373–2385.

Tuovinen, J.-P., D. Simpson, T. N. Mikkelsen, L. D. Emberson, M. R. Ashmore, M. Aurela, H. M. Cambridge, M. F. Hovmand, N. O. Jensen, T. Laurila, K. Pilegaard, and H. Ro-Poulsen (2001). Comparison of measured and modelled ozone deposition to forests in Northern Europe. *Water, Air and Soil Pollution, Focus*.

UNECE, United Nations Economic Commission of Europe (2009). Long-range Transboundary Air Pollution. Accessed January 2009. *http* : *//www.unece.org/env/lrtap/*.

Wang, X., G. Charmichael, D. Chen, Y. Tang, and T. Wang (2005). Impact of different emission sources on air quality during March 2001 in the Pearl River Delta(PRD) region. *Atmospheric Environment* (39), 5227–5241.

World Resources Institute, W. (2007). Climate and Atmosphere. Earth Trends, The Environmental Information Portal . Accessed May 2009. *http* : *//earthtrends.wri.org/*.

Wu, P.-M. and K. Okada (1994). NATURE OF COARSE NITRATE PARTICLES IN THE ATMOSPHERE - A SINGLE PARTICLE APPROCH. *Atmospheric Environment*.

Zhang, R., Z. Han, T. Cheng, and J. Tao (2009). Chemical properties and origin of dust aerosols in Beijing during springtime. *Particuology*, 61–67.